European Journal of Taxonomy 1043: 1–32
https://doi.org/10.5852/ejt.2026.1043.3203
europeanjournaloftaxonomy.eu
ISSN 2118-9773
2026 · Delicado D. *et al.*

Received: 15 July 2025 • *Accepted: 22 December 2025* • *Published: 24 February 2026*

Topic editor: Magalie Castelin • *Section editor: Thierry Backeljau* • *Desk editor: Pepe Fernández*

Research article
urn:lsid:zoobank.org:pub:DAF07C3F-ADB4-4D0A-873E-0A4D1CB260CB

Taxonomic assessment of 24 hydrobiid species (Caenogastropoda, Truncatelloidea) of conservation concern in springs of Iberia and Maghreb

Diana DELICADO [1,*], Jonathan P. MILLER [2], Khadija BOULAASSAFER [3], Marian A. RAMOS [4] & Torsten HAUFFE [5]

[1,2]Museo Nacional de Ciencias Naturales (MNCN-CSIC), José Gutiérrez Abascal 2, 28006 Madrid, Spain.
[3]Muséum d'Histoire Naturelle de Marrakech, Cadi Ayyad University, Prince Moulay Abdellah Boulevard, B.P. 2390, 40000 Marrakesh, Morocco.
[4]Deceased [3 March 2023]. Former address: Museo Nacional de Ciencias Naturales (MNCN-CSIC), José Gutiérrez Abascal 2, 28006 Madrid, Spain.
[5]Department of Biology, University of Fribourg, Chemin du Musée 10, CH-1700 Fribourg, Switzerland.

[*]Corresponding author: diana.delicado@mncn.csic.es
[2]Email: jonathanmiller@mncn.csic.es
[3]Email: khadija.boulaassafer@gmail.com
[5]Email: torsten.hauffe@ikmail.com

Abstract. *Corrosella* (family Hydrobiidae) represents one of the most diverse and threatened groups of spring snails in the Iberian Peninsula and Maghreb. Accurate delineation of species boundaries and understanding their geographic distributions are critical for effective conservation. However, inconsistent criteria used to define the 25 currently recognised species have led to considerable taxonomic uncertainty. This study presents a systematic revision of 24 species of *Corrosella* through an integrative approach combining multilocus phylogenies, morphometric analyses of shells and anatomical traits, and ecological characterisation, with comprehensive datasets for 22 species. Molecular and morphological evidence support the synonymisation of *C. navasiana*, *C. collingi*, *C. tajoensis*, *C. valladolensis valladolensis*, and *C. segoviana* under the earliest available name *C. navasiana*. Furthermore, we formally describe *C. ballestae* Delicado & Ramos sp. nov., a previously unrecognised species, and provide a redescription of the taxonomically complex *C. hinzi*. Despite a pronounced DNA sequence divergence among most species, morphological and ecological traits show significant overlap, underscoring the indispensable role of molecular data in resolving species diversity. These taxonomic updates refine the classification of *Corrosella*, elucidate species distributions, and establish a robust framework to support future research and conservation strategies.

Keywords. *Corrosella*, phylogeny, freshwater gastropods, Mediterranean region, species delimitation.

Delicado D., Miller J.P., Boulaassafer K., Ramos M.A. & Hauffe T. 2026. Taxonomic assessment of 24 hydrobiid species (Caenogastropoda, Truncatelloidea) of conservation concern in springs of Iberia and Maghreb. *European Journal of Taxonomy* 1043: 1–32. https://doi.org/10.5852/ejt.2026.1043.3203

Introduction

Snails belonging to the genus *Corrosella* Boeters, 1970 (family Hydrobiidae Stimpson, 1865) are widely distributed across the Iberian Peninsula in Europe, extending into southern France, and the Maghreb region of northwest Africa (Boulaassafer *et al.* 2021). These small animals (2.5–5.0 mm in shell length) predominantly inhabit mountain springs and streams, thriving at elevations between 500 and 1500 m (Delicado *et al.* 2012), with occasional records above 2000 m (Boeters *et al.* 2015). *Corrosella* is recognised as one of the most species-rich genera of freshwater snails in the mountain spring ecosystems of these regions, encompassing numerous narrowly distributed species. Exploring uncharted territories in the Betic (southeastern Iberia) and Rif (western Maghreb) Cordilleras offers the potential to discover additional undescribed species. However, describing and naming new species requires a solid taxonomic framework to ensure consistency in future classifications. Given the challenges posed by their small size, simple anatomy and inconspicuous shells, the identification of species of *Corrosella* often relies on DNA markers (Delicado & Ramos 2012; Delicado *et al*. 2012). Nevertheless, disparate morphological, anatomical and molecular criteria have been employed to define species boundaries within the genus (Boeters *et al.* 2015; Boulaassafer *et al.* 2021; Martín-Álvarez *et al.* 2024), resulting in a taxonomic landscape fraught with ambiguity. Incorporating multiple criteria promises to furnish a cohesive taxonomic scheme, facilitating species classification and informing conservation strategies.

The taxonomic history of *Corrosella* has undergone multiple revisions since Boeters (1970) first described the genus based on anatomical characteristics, such as the elongated, folded bursa copulatrix and the absence of an appendix on the mantle margin. *Corrosella falkneri* Boeters, 1970 was designated as the type species. Originally recognised as a distinct genus, *Corrosella* was later reclassified as a subgenus of *Pseudamnicola* Paulucci, 1878, due to similarities in bursa shape and its occurrence at the western periphery of the range of *Pseudamnicola* (Boeters 1984). This and subsequent work by Boeters (1984, 1986) led to the description of two new species based on shell and anatomical features: *Pseudamnicola* (*Corrosella*) *luisi* Boeters, 1984 and *Pseudamnicola* (*Corrosella*) *hinzi* Boeters, 1986, the latter being known only from its type locality in Bulbuente, Zaragoza Province and two springs in Burgos Province, Spain. In a comprehensive study of hydrobiid snails in Spain and Portugal, Boeters (1988) included these species and transferred *Amnicola navasiana* Fagot, 1907 to the subgenus. He also clarified the type locality of *P.* (*C.*) *hinzi* as Balsa de Vargas in Bulbuente, Zaragoza. Delicado *et al.* (2010) also identified two *P.* (*C.*) *hinzi* populations in Teruel Province, Spain. Boeters (1999) described the first subterranean species of the subgenus, *P.* (*C.*) *hydrobiopsis* Boeters, 1999, based on three empty shells collected from a spring in Granada Province, Spain. He observed that the shell of this species was more slender and had taller spires than that of other members of the subgenus, suggesting a potential affinity with the conic-shaped genus *Hydrobia* Hartmann, 1821. However, Boeters (1999) also highlighted the corroded shell apex, a characteristic feature of *Corrosella*, supporting its attribution to this genus.

The application of molecular techniques has been pivotal in addressing the limitations of morphology-based taxonomy in *Corrosella*. Delicado *et al.* (2012) conducted the first molecular phylogenetic analysis using the cytochrome *c* oxidase subunit I (COI), confirming the distinctiveness of previously described species and leading to the discovery of five novel species in southern Iberia. These findings underscore the prevalence of cryptic diversity within the genus and demonstrate the necessity of integrating DNA sequence data for reliable species delimitation. A subsequent phylogenetic study with an expanded geographic scope revealed that populations from the eastern Iberian Peninsula, previously attributed to the French species *Pseudamnicola* (*Corrosella*) *astierii* (Dupuy, 1851) by Gasull (1981), actually

represent an endemic species, provisionally named *Pseudamnicola* (*Corrosella*) *hauffei* Delicado & Ramos, 2012 (Delicado & Ramos 2012). This species was described using shell morphology, COI sequences and anatomical features. Martínez-Ortí (2018) later observed that the shell dimensions of the cave species *Neohoratia herreroi* Bech, 1993 were similar to those of *P.* (*C.*) *hauffei*, leading to the conclusion that it represents the same taxon, properly referred to as *Pseudamnicola* (*Corrosella*) *herreroi* (Bech, 1993). Further multilocus phylogenetic analysis expanded COI sequencing of previously sampled populations and included new populations from central Iberia, then assigned to *P.* (*C.*) *navasiana* and *P.* (*C.*) *hinzi* (Delicado *et al.* 2013). That study identified 11 distinct clades corresponding to the nominal species of the subgenus and one additional clade provisionally referred to as *Pseudamnicola* (*Corrosella*) sp., which was also included in subsequent molecular phylogenies of the group (Delicado *et al.* 2015; Boulaassafer *et al.* 2021). The analysis further revealed that populations of *P.* (*C.*) *hinzi* from Burgos Province belong to the *P.* (*C.*) *navasiana* clade, implying a broader distribution of *P.* (*C.*) *navasiana* across central and northern Iberia, rather than being restricted to Zaragoza Province (northwestern Spain). Delicado *et al.* (2013) also confirmed that *P.* (*C.*) *hinzi*, identified as an old lineage within the subgenus, is a taxon with a limited distribution, occurring exclusively in the Spanish provinces of Zaragoza and Teruel.

Based on molecular and morphological evidence, *Pseudamnicola* (*Corrosella*) was elevated to full genus rank (Delicado *et al.* 2015). Boeters *et al.* (2015) corroborated these morphological differences. Moreover, these authors proposed recognising three subclades within the *P.* (*C.*) *navasiana* clade, identified by Delicado *et al.* (2013), as valid species. Despite minimal genetic differences – a rarity among species of *Corrosella* – substantial morphological variations in shell and genital anatomy were observed among individuals from the type localities of these three potentially distinct species. In contrast to Delicado *et al.* (2013), this revised species scheme suggests that the *P.* (*C.*) *navasiana* clade comprises three narrowly endemic species, significantly reducing the known geographic range of the original species. Additional research and subsequent studies have identified two more endemic species of *Corrosella* within the previously defined range of the *P.* (*C.*) *navasiana* complex, as well as one in southern France, based on morphological data (Boeters *et al.* 2015; Talaván-Serna & Talaván-Gómez 2019). On this basis, the *P*. (*C.*) *navasiana* complex may comprise six species in total.

Boulaassafer *et al.* (2021) extended previous molecular phylogenies to include Moroccan populations, identifying a clade comprising six putative species on the African side of the Strait of Gibraltar. Recently, Talaván-Serna & Talaván-Gómez (2024) described the first fossil species of the genus, *Corrosella arlanzonica* Talaván-Serna & Talaván-Gómez, 2024, from the middle Miocene (around 10 Ma) in central Iberia and Martín-Álvarez *et al.* (2024) an additional extant species from southern Iberia, bringing the total number of species in the genus to 25 (24 living and one extinct species; MolluscaBase eds. 2025). However, given the gradual decline in morphological divergence towards the present, resulting in closely related species appearing morphologically similar (Delicado *et al.* 2018), species described solely based on morphology – primarily from the type locality – require re-evaluation within a comprehensive genus-wide context. This re-evaluation should consider intraspecific variation in both morphological and molecular characters.

Despite advances in understanding *Corrosella* diversity, many species remain poorly studied, particularly in terms of their conservation status. A few species are listed in regional conservation plans: *C. falkneri* and *C. hydrobiopsis* are listed as 'Vulnerable,' and *C. luisi* as 'Near Threatened' in the *Libro Rojo de los Invertebrados de Andalucía* (Barea-Azcón *et al.* 2008). Additionally, *C. hinzi* is classified as 'Endangered' in the *Catálogo de Especies Amenazadas de Aragón* (Alcántara de la Fuente 2007). Nine species have been assessed by the International Union for Conservation of Nature (IUCN) Red List, with the majority considered at risk (IUCN 2024). However, the narrow distributions and vulnerability to habitat changes, such as those caused by climate change and human activities (Álvarez-Halcón *et al.*

2012; Boulaassafer *et al.* 2023), emphasise the urgent need for accurate taxonomic frameworks to inform conservation strategies.

Taxonomic and systematic studies, especially those employing holistic approaches, have been crucial in defining management units for gastropod conservation (Perez & Minton 2008). This study aims to revise the taxonomy of 24 species of *Corrosella* – 23 previously recognised taxa and one undescribed species (*Pseudamnicola* (*Corrosella*) sp.) first detected by Delicado *et al.* (2013) – through a holistic approach. Of these, 22 species were represented by ethanol-preserved material suitable for molecular and anatomical analyses, while *C. hydrobiopsis* and *C. tejedoi* (Boeters, Callot-Girardi & Knebelsberger, 2015) were available only as empty shells. We utilise multilocus sequence data, shell morphology, anatomical measurements, and ecological information to validate species across multiple populations, including those beyond the type localities. Our analyses address intraspecific variation and propose synonymies where appropriate, and we formally describe a previously unrecognised species based on these results. These taxonomic updates are crucial for refining the genus's classification, clarifying the geographic distribution of species, and informing conservation efforts for these threatened freshwater snails.

Material and methods

Data compilation

We compiled DNA sequence, morphological and ecological data from 62 populations of *Corrosella* snails, representing 22 putative species (21 formally described and one informally recognised) collected from spring habitats across the genus' geographical range (Supp. file 1: Table S1). For most species, we used existing morphological and DNA sequence data from previous studies (Delicado & Ramos 2012; Delicado *et al.* 2012, 2013; Boulaassafer *et al.* 2021). New morphological and anatomical data were obtained for *C. hinzi*, *C. navasiana*, *C. collingi* (Boeters, Callot-Girardi & Knebelsberger, 2015) and *C. tajoensis* (Boeters, Callot-Girardi & Knebelsberger, 2015), based on samples previously collected and sequenced (Delicado *et al.* 2013), housed in the Malacology Collection at the Museo Nacional de Ciencias Naturales (MNCN-CSIC). Additionally, we generated new anatomical and DNA sequence data for topotypical specimens of *C. segoviana* (Talaván-Serna & Talaván-Gómez, 2019) and for specimens collected near the type locality of *C. valladolensis valladolensis* (Boeters, Callot-Girardi & Knebelsberger, 2015) at Aceña Spring in Quintanilla de Onésimo, located ca 300 m from the type locality Arca Spring in the same village (see Systematic section). Samples of these two species were collected manually from stones, fixed according to Araujo *et al.* (1995), stored in 80% ethanol, and deposited at the MNCN-CSIC. Shell samples of the subterranean *C. hydrobiopsis* and *C. tejedoi* were also included in our morphometric analyses using images from Delicado *et al.* (2012) and Boeters *et al.* (2015), respectively; however, no sequence data are available for these species, as only empty shells were collected.

DNA sequence data and phylogenetic inference

We conducted DNA sequencing on 2 specimens from each *C. segoviana* and *C. valladolensis* population (GenBank accession numbers provided in Supp. file 1: Table S1) to augment a previously published *Corrosella* dataset (Boulaassafer *et al.* 2021). Genomic DNA was extracted using the DNeasy Blood and Tissue Kit (QIAGEN, Hilden, Germany) from a small piece of foot tissue. Fragments of two mitochondrial genes, cytochrome *c* oxidase subunit I (COI) and 16S rRNA (16S), and one nuclear gene, 28S rRNA (28S), were amplified using the primer pairs, PCR mix and cycling conditions described by Miller *et al.* (2022). PCR products were sequenced by the Macrogen Service Centre (Madrid, Spain). Forward and reverse sequences were assembled and edited using SEQUENCHER ver. 4.6 (Gene Codes, Ann Arbor, MI), then aligned alongside GenBank sequences in MEGA ver. 11.0.10 (Tamura *et al.* 2021) to produce three gene-specific matrices. We selected the outgroup species *Pseudamnicola subproductus* (Paladilhe, 1869) (subfamily Pseudamnicolinae), *Peringia ulvae* (Penant, 1777) (related subfamily Hydrobiinae) and

Mercuria similis (Draparnaud, 1805) (subfamily Mercuriinae) according to the phylogenetic framework of Delicado *et al.* (2024). COI gene alignment was performed manually, while ribosomal DNA fragments were aligned using MAFFT ver. 7.402 (Katoh & Standley 2013) with default gap penalty settings. Hypervariable regions of the 16S and 28S alignments were filtered using Gblocks ver. 0.91b (Castresana 2000) via the Gblocks web server (http://phylogeny.lirmm.fr/phylo_cgi/one_task.cgi?task_type=gblocks). Mean sequence divergences for COI (measured as uncorrected pairwise distances) were calculated using MEGA. The optimal substitution model for each gene partition was identified using jModelTest ver. 2.1.7 (Darriba *et al.* 2012) based on the corrected Akaike information criterion (Akaike 1974).

Phylogenetic relationships were inferred using concatenated alignments of the three genes, with outgroups, applying maximum likelihood (ML) and Bayesian inference (BI) methods. ML analysis was performed with RAxML-NG ver. 1.0.2 (Kozlov *et al.* 2019), starting with 200 random trees and applying the substitution models for each gene partition as determined by jModelTest. Transfer bootstrap expectation (TBE) and Felsenstein bootstrap (FB) values were calculated using the autoMRE criterion (cutoff: 0.03) and up to 5000 bootstrap replicates. For BI, phylogenies were generated using MrBayes ver. 3.2.7a (Ronquist *et al.* 2012) with two independent Markov chain Monte Carlo (MCMC) runs of 5 million generations, sampling trees every 1000 generations and discarding the first 10% as burn-in. Separate mixed substitution models were applied to each partition in all BI analyses. Convergence was confirmed by ensuring split frequency standard deviations fell below 0.01, and posterior probabilities (BPPs) provided support for the resulting phylogenies. Tree topology and branch support values were visualised in FigTree ver. 1.4.3 (Rambaut 2016). Additionally, two supplementary phylogenetic analyses were performed using a COI-only matrix to incorporate *Corrosella piti* Martín Álvarez, Glöer, López-Soriano, Raven, Á. Alonso, O. Sánchez & Quiñonero-Salgado, 2024 (for which only COI sequences are available in GenBank: PP667386 and PP667387; Martín-Álvarez *et al.*, 2024). These analyses were conducted in RAxML-NG and MrBayes under the same settings and model selection procedures described above.

Molecular species delimitation methods

Species delimitation based on DNA was performed using three methods. First, we applied the Assemble Species by Automatic Partitioning (ASAP) method (Puillandre *et al.* 2021), via the ASAP web server (https://spartexplorer.mnhn.fr/delimitation), analysing COI sequences after removing identical haplotypes and outgroup sequences. The analysis employed uncorrected distances while retaining the default settings for all other parameters.

Tree-based methods included the generalized mixed Yule-coalescent (GMYC) model (Pons *et al.* 2006) and the Poisson tree processes (PTP) model (Zhang *et al.* 2013). For GMYC, we employed the single-threshold version (stGMYC; Reid & Carstens 2012), using ultrametric trees generated in BEAST ver. 2.6.6 (Bouckaert *et al.* 2019) based on the mitochondrial dataset, excluding outgroups. bModelTest ver. 1.2.1 (Bouckaert & Drummond 2017) inferred the optimal substitution models. A strict clock rate of 1.0 was applied for all loci under a birth-death model tree prior (Gernhard 2008), with 10 random starting seeds and chain lengths set to 15 million generations, sampling parameters every 5000 steps. We used Tracer ver. 1.7.2 (Rambaut *et al.* 2018) to confirm that all parameters had an effective sample size greater than 200. The maximum clade credibility (MCC) tree was generated using TreeAnnotator after excluding the initial 10% of the sampled trees. This tree and 100 random post-burn-in phylogenies from the same analysis served as input for stGMYC, following the removal of zero-length branches (i.e., identical haplotypes) with the R package ape ver. 5.0 (Paradis & Schliep 2019), for the R statistical programming environment ver. 4.1.3 (R Core Team 2025). The stGMYC analysis was performed using the R package bGMYC ver. 1.0.2 (Reid 2014), running for 100 000 MCMC generations and sampling every 100th generation after a burn-in period of 10 000 generations.

For PTP, we applied both the Bayesian variant (bPTP; Zhang *et al.* 2013) and the maximum likelihood multi-rate (mPTP; Kapli *et al.* 2017) methods, both requiring a non-ultrametric phylogenetic tree as input. We generated this tree using RAxML-NG, based on our mitochondrial dataset and the substitution models selected by jModelTest. The analysis began with 200 random starting trees. To assess branch support, we employed the transfer bootstrap expectation method, applying the autoMRE bootstrapping convergence criterion (cut-off: 0.030) with a maximum of 5000 bootstrap replicates. Before executing the PTP analyses, we removed outgroup taxa from the optimal tree using the R package ape. We performed the bPTP and mPTP delimitations using mPTP ver. 0.1.1 (Kapli *et al.* 2017), employing the same phylogenetic tree while setting the minimum branch length to 0.000942 to eliminate duplicated haplotypes. The MCMC analysis for bPTP was executed for 200 million generations, with sampling conducted every 2 million generations, while discarding the initial 50 million generations. To evaluate convergence, we examined the trace plot of log-likelihood against generation.

Morphometric variables and analyses

Morphometric variables included shell shape coordinates, seven linear measurements and one size-related ratio for shell dimensions, nine measurements of the female genitalia and five measurements of the male genitalia (see Supp. file 1: Table S2). Shell measurements were recorded for 791 adult individuals (mean 32 individuals, range 1–127 individuals per species), including type specimens of *C. collingi*, C. *tajoensis*, *C. valladolensis*, *C. tejedoi and C. segoviana* depicted in Boeters *et al.* (2015) and Talaván-Serna & Talaván-Gómez (2019). Due to differences in resolution, most of the latter images were not utilised for the shell shape analyses, conducted on 778 shells. Anatomical data were obtained from 294 adult individuals (Supp. file 1: Table S1). Following shell dissolution in EDTA (ethylenediaminetetraacetic acid), specimens of the newly characterised species were dissected and photographed using an AF M205 FA stereo microscope equipped with a digital camera (Leica Microsystems, Wetzlar, Germany). Radulae were extracted from the buccal mass using the initial step of a CTAB protocol for DNA isolation (Wilke *et al.* 2006). Post-drying, radulae, opercula and shells were mounted on metallic stubs and sputter-coated with gold for 50 seconds, then photographed using the field emission scanning electron microscopes (FESEM) Philips Quanta 200 and FEI INSPECT (FEI Company, the Netherlands). Anatomical terminology adhered to Hershler & Ponder (1998), with the number of spire whorls counted following Ramos *et al.* (2000). The central nervous system concentration was quantified using the right pleural ganglion (RPG) ratio as described by Davis *et al.* (1976).

For shell shape variation analysis, images of 778 adult shells were digitised with tpsDig2 ver. 2.32 (Rohlf 2021), incorporating 11 landmarks and five open semi-landmark curves as delineated in Delicado *et al.* (2025). The semi-landmarks were aligned along their curves with the SemiLand8 tool within the CoordGen8 program, part of the Integrated Morphometrics Package (IMP) software suite (Sheets 2014). The aligned shape coordinates were then analysed in MorphoJ ver. 1.07a (Klingenberg 2011). Procrustes superimposition was applied to generate a consensus shell shape for all individuals in the dataset, separating shape from size (i.e., centroid size). A multivariate regression of Procrustes coordinates onto centroid size, with 10 000 randomisation rounds, tested the effect of size on shape. No significant effect of size on Procrustes variance was found (% predicted = 0.09, $p = 0.59$), indicating that shape correction for allometry was unnecessary. Principal component analysis (PCA) was performed on the variance-covariance matrix to reduce dimensionality. The first five components accounted for 81% of the cumulative variation and were used as new shape variables for subsequent validation analyses.

The species discriminating power of four datasets was tested: shell shape variables and linear measurements from the shell, female genitalia and male genitalia. Missing data, which accounted for less than 10% due to factors such as broken anatomical structures, were substituted with estimated values using random forest imputation via the R package missForest ver. 1.5 (Stekhoven & Bühlmann 2012). To stabilise variance, we applied a logarithmic transformation to the linear data. Species validation was

conducted through eight canonical variate analyses (CVA) using Past ver. 4.09 (Hammer *et al.* 2001). Each variable set was tested for two species groupings: one including all species and another focusing solely on the species of Clade 1 (see taxonomic groups in Fig. 1).

Ecological data

We collected 13 ecological parameters classified into three categories: topography, hydroclimate and soil. Four topographic variables (i.e., Elevation, Slope, Topographic Position Index and Terrain Ruggedness Index) were extracted from Shuttle Radar Topography Mission (SRTM) elevation data (3 arcseconds) via QGIS ver. 3.18.1 (QGIS Development Team 2023). Three variables representing flow condition (upstream/downstream flow length and accumulation) were sourced from HydroSHEDS ver. 1 (https://www.hydrosheds.org; Lehner *et al.* 2008; Hengl *et al.* 2014). Four hydroclimate variables (Annual Mean Upstream Temperature, Upstream Temperature Annual Range, Annual Upstream Precipitation and Upstream Precipitation Seasonality) were obtained from EarthEnv (https://www.earthenv.org/streams; Domisch *et al.* 2015), which derived these parameters from the Bioclim framework (see https://worldclim.org/bioclim for details). Soil data on organic carbon (g/kg) and pH were also extracted from EarthEnv. To explore ecological variation across species, a PCA was conducted on the log-transformed ecological variables using Past ver. 4.09.

Collection abbreviations

BOE = Boeters collection, Munich, Germany
MNCN = Museo Nacional de Ciencias Naturales (CSIC), Madrid, Spain
SMF = Forschungsinstitut und Natur-Museum Senckenberg, Frankfurt a. M., Germany

Results

Phylogenetic analyses and molecular species delimitation

The ML and BI analyses of the concatenated dataset (2107 bp) yielded congruent topologies with high support for most key nodes, particularly those defining species and interspecific relationships. As a result, only the Bayesian topology is presented in Fig. 1, with the ML results available in Supp. file 2: Fig. S1. Both analyses consistently resolved six major clades within the genus (BPP > 0.95, TBE > 0.90 and FB > 75%), encompassing 18 species-level clades for the nominal species and one informally recognised taxon within Clade 5 (Fig. 1). However, *C. navasiana*, *C. valladolensis* and *C. segoviana* were not recovered as distinct species-level clades; their specimens, including topotypic ones, are intermixed within a moderately supported group (BPP = 0.90, TBE = 0.87 and FB = 62%). Individuals of *C. tajoensis* did not form a monophyletic group. TBE support values in the ML analysis were generally higher than FB support values. *Corrosella hinzi* clustered closely with south Iberian species (BPP = 0.91, TBE = 0.89 and FB = 55%), while the phylogenetic placement of *C. nechadae* Boulaassafer, Ghamizi & Delicado, 2021 was unresolved in BI but supported in the ML analysis with a TBE value of 0.96. In the COI-only analyses, *C. piti* clustered within Clade 5 as the sister lineage to *C. iruritai* (Delicado, Machordom & Ramos, 2012), with strong support (BPP = 0.95, TBE = 0.84, FB = 70%), and was placed relatively distant from the newly described *C. ballestae* Delicado & Ramos sp. nov. (Supp. file 2: Fig. S2).

The ASAP analysis identified 20 groups, of which 16 corresponded to taxonomically recognised species and one to a previously identified but undescribed clade. Both versions of the PTP method yielded 19 groups, aligning with the ASAP scheme but combining *C. andalusica* (Delicado, Machordom & Ramos, 2012) with the undescribed clade. The stGMYC analysis recovered 21 groups, following the ASAP pattern but subdividing the *C. andalusica* cluster into two. In all analyses, *C. navasiana*, *C. collingi*, *C. tajoensis*, *C. valladolensis* and *C. segoviana* were consistently merged, whereas *C. bareai* (Delicado, Machordom & Ramos, 2012) and *C. manueli* (Delicado, Machordom & Ramos, 2012) were divided into two distinct groups.

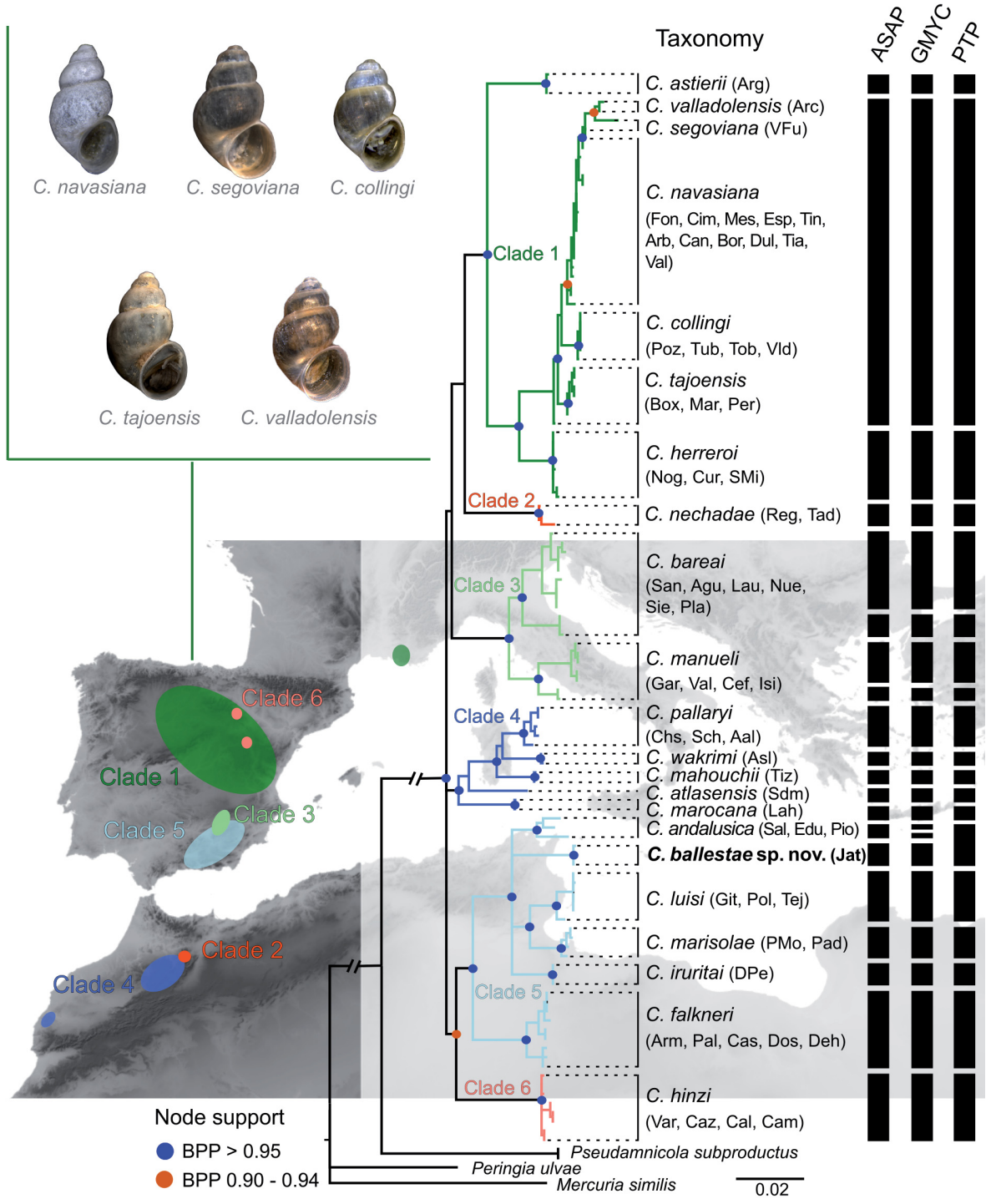

Fig. 1. Bayesian phylogeny of species of *Corrosella* Boeters, 1970 based on a concatenated dataset of COI, 16S and 28S sequences. Bayesian posterior probabilities >0.90 are indicated at nodes above the species level. Vertical bars on the right denote groups identified by molecular delimitation methods: Assemble Species by Automatic Partitioning (ASAP), the single-threshold generalized mixed Yule-coalescent (GMYC) model and the Bayesian Poisson Tree Processes (PTP) method. Major clades are distinguished by colour coding, with an inset showing their geographic distribution and representative photo vouchers for species within Clade 1. Species names are followed by locality codes, detailed in Supp. file 1: Table S1. Scale bar below the topology: substitutions per site.

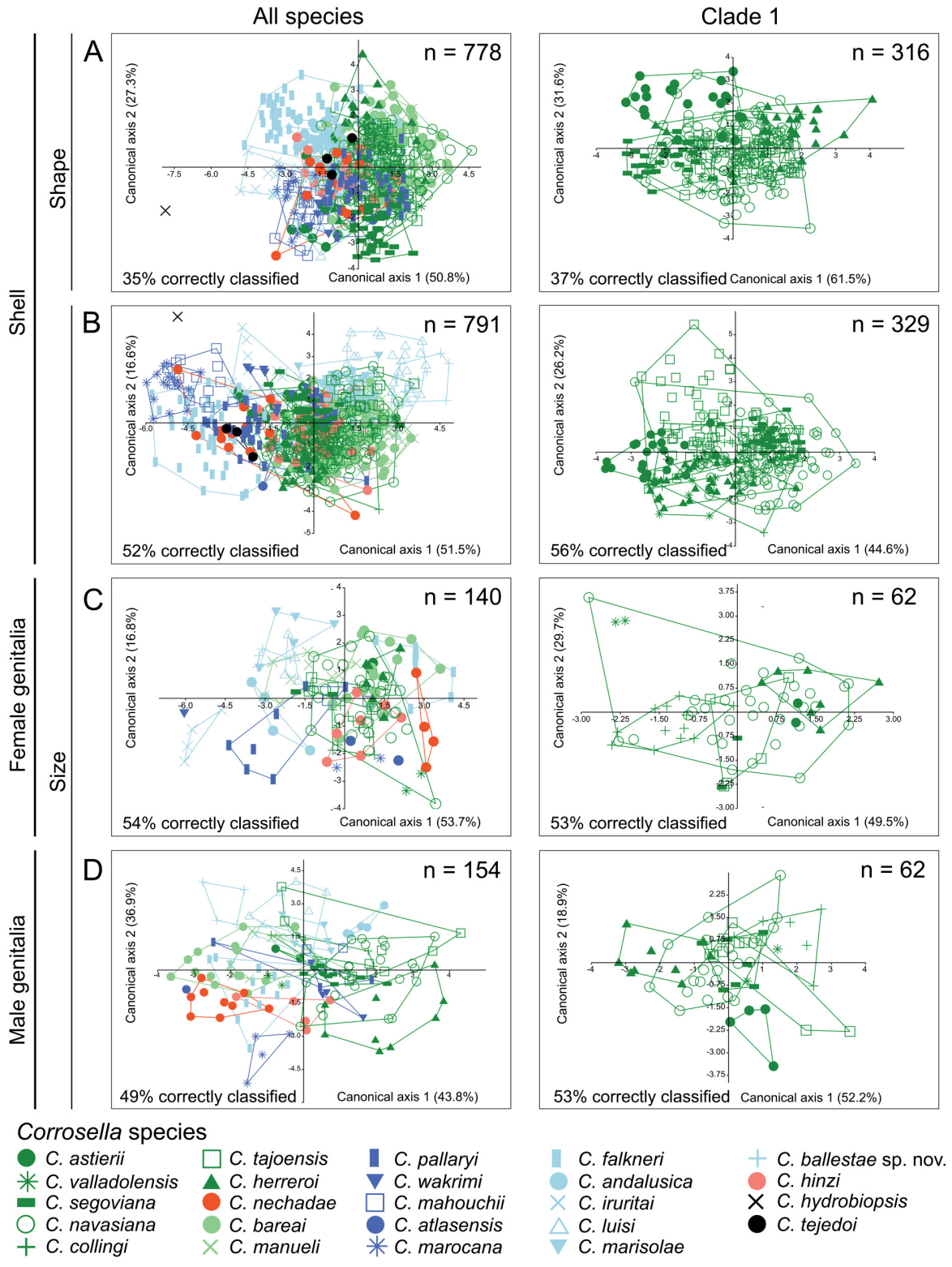

Fig. 2. Morphological differentiation among species of *Corrosella* Boeters, 1970. The left column shows canonical variate analysis (CVA) results for all species across the major clades, while the right column focuses on species within Clade 1. Analyses were conducted using four datasets. **A**. Principal components of shell shape. **B**. Shell measurements. **C**. Female genitalia measurements. **D**. Male genitalia measurements. The sample size (n) for each dataset is provided in the top right corner of each plot.

Morphological differentiation among species

CVA based on 24 a priori-defined species successfully classified 35% of individuals by shell shape and 52% by shell size, with shell length/width ratio and shell length as primary influences. Although the convex hulls of species largely overlapped in both analyses, *C. falkneri* and *C. iruritai* displayed clearer differentiation in shell shape. Notably, only the holotype of *C. hydrobiopsis* was positioned outside the morphospace for both shell shape and size (Fig. 2A–B). Species within Clade 1 (composed of *C. navasiana*, *C. collingi*, *C. tajoensis*, *C. valladolensis* and *C. segoviana*) could not be distinguished by

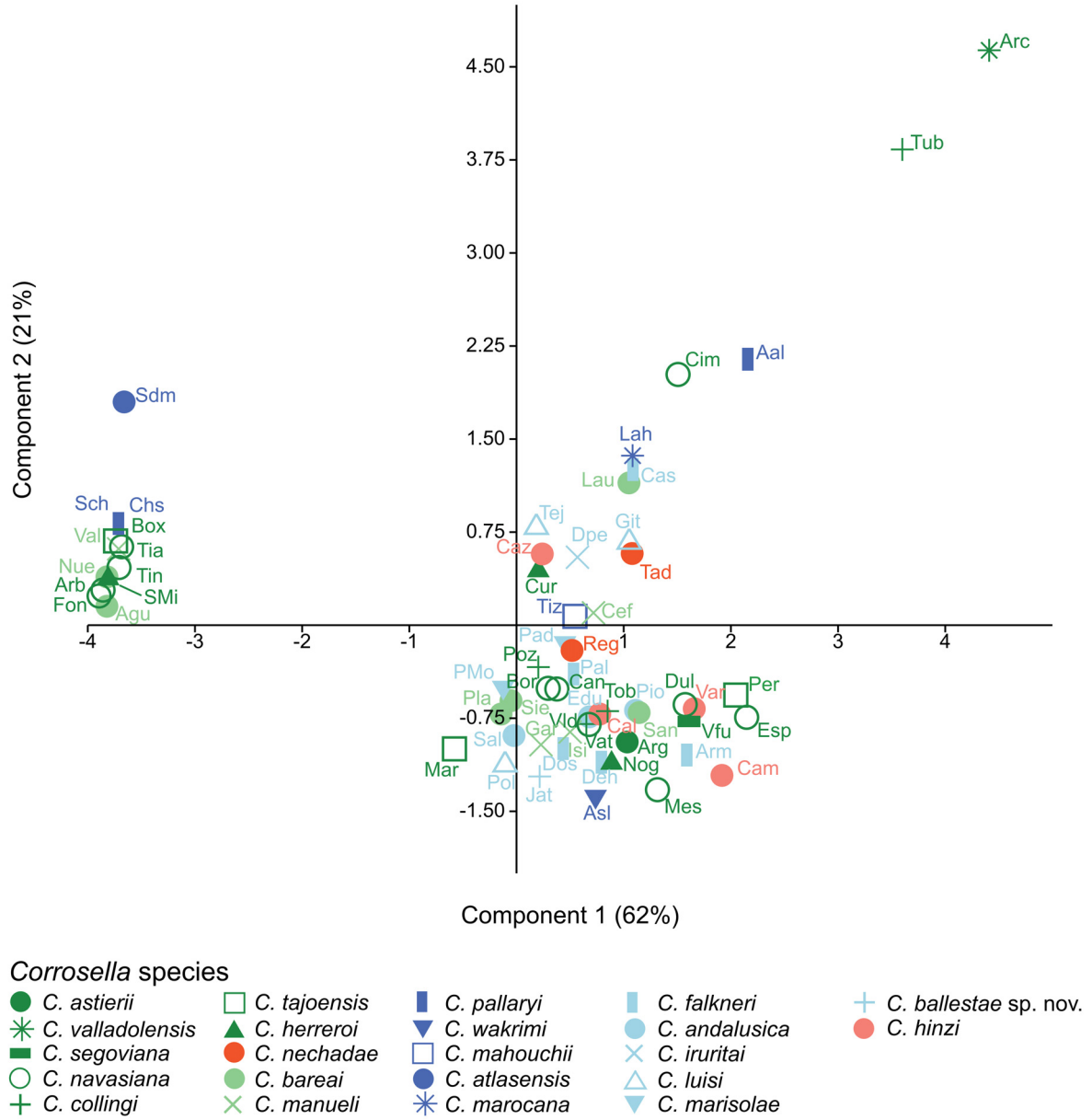

Fig. 3. Principal Component Analysis (PCA) of 13 ecological variables across *Corrosella* Boeters, 1970 populations analysed in this study. Each point represents a population, labelled with locality codes (detailed in Supp. file 1: Table S1) and colour-coded according to major clades (see Fig. 1). The percentage of variance explained by each principal component is indicated in parentheses.

shell shape or size, with the variables accounting for only 37% and 56% of the variation among species groups, respectively.

Similarly, female and male genitalia variables were generally ineffective for species discrimination, correctly classifying 54% and 49% of individuals across the 24 studied species, respectively (Fig. 2C–D). Female individuals clustered mainly in a restricted region of the morphospace. In contrast, *C. wakrimi* Boulaassafer, Ghamizi & Delicado, 2021 and *C. iruritai* showed clearer separation from this cluster due to their shorter bursa copulatrix and bursal duct, which accounted for most of the variation in both canonical functions. In the morphospace based on male genitalia variables, most species hulls overlapped, with only *C. marocana* (Pallary, 1922) and *C. ballestae* sp. nov. showing a clear differentiation based on the penis width and length, which were the most discriminant variables in the first and second canonical functions.

Within Clade 1, *C. navasiana* exhibited high variability in genitalia features, overlapping with the morphospaces of other species in the clade. The width of the pallial oviduct and length of the bursa copulatrix explained most of the variation in female genitalia, while the penis length and the penis length/head length ratio were key for male genitalia differentiation.

Ecological characteristics

PCA revealed that three ecological variables – flow accumulation (i.e., the upstream drainage area of the locality), flow length upstream (i.e., distance from the furthest river source upstream) and annual upstream precipitation – were the primary factors explaining variation among populations of *Corrosella*, accounting for 81% of total variance. In the first principal component, all three variables were positively correlated. In the second component, flow length upstream was negatively correlated, contrasting with positive correlations for the other two variables.

Most populations of *Corrosella* clustered near the origin of the ordination space (Fig. 3), reflecting similar preferences for these influential variables. Species with more than two sampled populations demonstrated broader habitat range, as seen in *C. navasiana*, *C. herreroi*, *C. pallaryi* (Ghamizi, Vala & Bouka, 1997), *C. bareai* and *C. manueli*. Other species, such as *C. hinzi*, *C. falkneri*, *C. marisolae* (Delicado, Machordom & Ramos, 2012) and *C. nechadae* showed more restricted habitat preferences. The most distinct populations belonged to *C. valladolensis valladolensis* and *C. collingi*, which are synonymised with *C. navasiana* in the systematic section below, suggesting this species can inhabit diverse water flow conditions and variable distances from river sources.

Systematics

Class Gastropoda Cuvier, 1795
Subclass Caenogastropoda Cox, 1960
Order Littorinimorpha Golikov & Starobogatov, 1975
Family Hydrobiidae Stimpson, 1865
Subfamily Pseudamnicolinae Boeters & Falkner, 2017
Genus *Corrosella* Boeters, 1970

Corrosella ballestae Delicado & Ramos sp. nov.
urn:lsid:zoobank.org:act:00C6B95A-52FD-4D28-9A6B-6333FD7A51E3
Figs 4–5

Pseudamnicola (*Corrosella*) sp. – Delicado *et al.* 2013: 391–392, figs 2–3,
Corrosella sp. – Boulaassafer *et al.* 2021: 399–400, figs 2–3. — Delicado *et al.* 2024: 90, fig. 2**.**

Diagnosis

Shell ovate-conic, large, with an inflated body whorl; upper region of shell aperture slightly pointed; protoconch microsculpture pitted; periostracum yellowish; central radular tooth formula 4-C-4/1-1; bursa copulatrix pyriform, U-shaped fold; seminal receptacle elongate with short peduncle; penis gradually tapering, with a patch of black pigment in distal region and a narrow base; nervous system pigmented, moderately concentrated (mean RPG ratio = 0.47); cerebral ganglia approximately equal in size.

Etymology

This species is named after Irene Ballesta, in recognition of her diligent collection of freshwater molluscs from numerous Andalusian localities, including specimens of this species.

Type material

Holotype

SPAIN • sex unknown (dry preserved, ESEM preparation); Granada, Gordo Spring near Játar; 36.9308° N, 3.9166° W; MNCN 15.05/63703H.

Paratypes

SPAIN – **Granada Province** • 10 specs (preserved in ethanol 96% and 3 processed for DNA sequencing); same collection data as for holotype; 1 Jun. 2009; I. Ballesta and J.M Barea-Azcón leg.; MNCN 15.05/63703P • 40 specs (preserved in ethanol 70% and 100%, 8 dissected); a pond connected to Gordo Spring; 36.9308° N, 3.9166° W; 1 Jun. 2009; I. Ballesta and J.M Barea-Azcón leg.; MNCN 15.05/63704 • 60 specs (preserved in ethanol 70%); a second pond connected to Gordo Spring; 36.9308° N, 3.9166° W; 1 Jun. 2009; I. Ballesta and J.M Barea-Azcón leg.; MNCN 15.05/63705.

Description

Shell. Ovate-conic, whorls about 5, height 4.25–5.50 mm (Fig. 4A–E); periostracum yellowish, often eroded, especially on early whorls; protoconch 1.5 whorls, diameter ca 450 µm, nucleus ca 150 µm wide (Fig. 4F); protoconch microsculpture pitted (Fig. 4G–H); teleoconch whorls convex, separated by a deep suture; last body whorl about ⅔ of total length; peristome orthocline, slightly pointed at upper region; inner lip thicker than outer lip, partially hiding the umbilicus; aperture margin simple, straight (Fig. 4E).

Operculum. Corneous, yellowish, thin, pliable, ellipsoidal, paucispiral with submarginal nucleus, 2.75 whorls; muscle attachment oval, located near nucleus (Fig. 5A–B).

Radula. Length intermediate (20% of total shell length), approximately 8 times as long as wide; having ca 55 rows of teeth. Central tooth formula 4-C-4/1-1, central cusp U or V-shaped, cutting edge slightly concave (Fig. 5C–D). Lateral tooth formula 3-C-3, central cusp U-shaped. Inner marginal teeth with 18–20 cusps; outer marginal teeth with 20–22 cusps (Fig. 5E).

Pigmentation and anatomy. Head dark brown, pigmented from snout to neck (Fig. 5K); neck paler; tentacles with central brown stripe; ocular lobes unpigmented; snout as long as wide, with pronounced distal lobation; foot of intermediate length, dorsal surface pigmented. Ctenidium located in the anterior region of the pallial cavity; 20–24 gill filaments, taller than wide. Osphradium intermediate in width, positioned opposite middle of ctenidium (Fig. 5F). Stomach slightly longer than wide; posterior chamber slightly larger than anterior (Fig. 5G); style sac longer than wide, encircled by intestine with a small brown patch.

Nervous system. Dark brown pigmentation, moderately concentrated (mean RPG ratio = 0.47); cerebral ganglia equal in size, darker than other ganglia and connectives; supraoesophageal connective ca 6 times as long as pleurosuboesophageal one (Fig. 5H).

Female genitalia. Capsule gland longer than albumen gland (Fig. 5I); bursa copulatrix pyriform with U-shaped fold; bursal duct shorter than bursa, partly or fully embedded in bursa copulatrix; renal oviduct black-pigmented to above seminal receptacle insertion, coiled; seminal receptacle elongate, with short duct, positioned slightly above the junction of bursal duct and renal oviduct (Fig. 5J).

Male genitalia. Prostate gland about 3 times as long as wide. Penis slightly pigmented distally, gradually tapering, attached to neck behind right eye; weak folds along inner edge; penial duct runs straight along outer side (Fig. 5K).

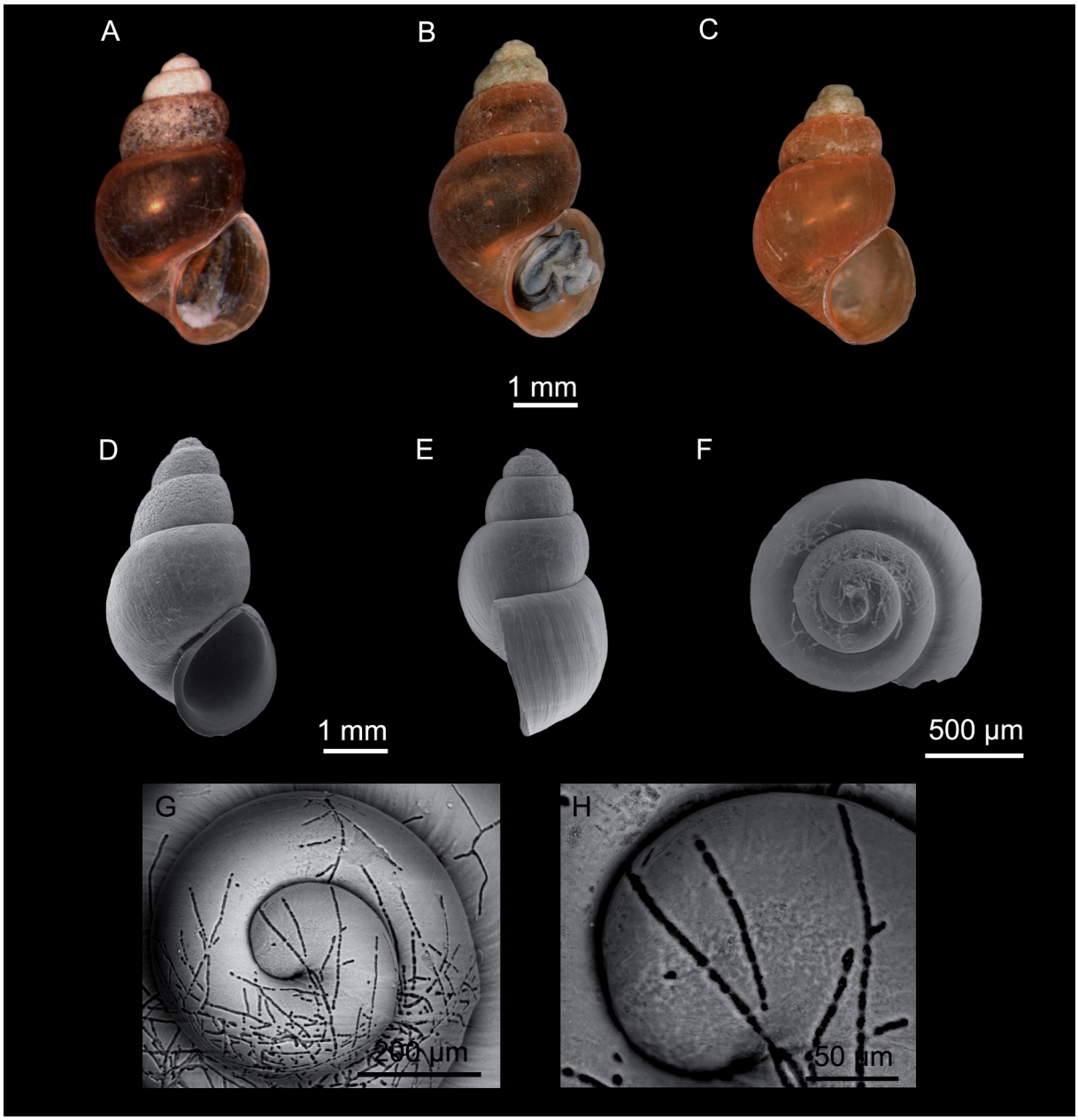

Fig. 4. Shells of *Corrosella ballestae* Delicado & Ramos sp. nov. **A–C, F–H**. Paratypes (MNCN 15.05/63703P). **D–E**. Holotype (MNCN 15.05/63703H), frontal and lateral views. **F–G**. Details of the protoconch. **H**. Protoconch microsculpture.

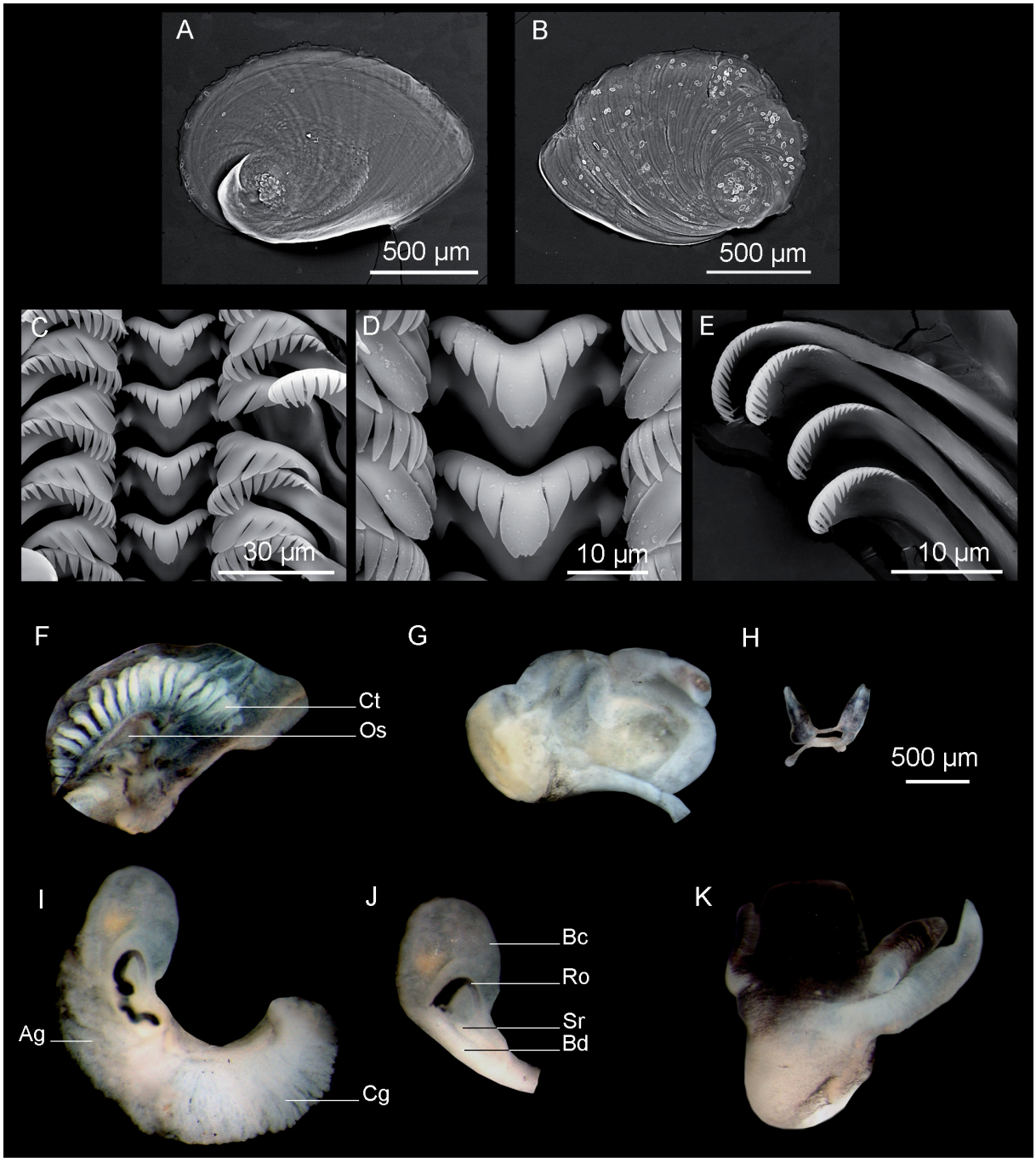

Fig. 5. Anatomy of *Corrosella ballestae* Delicado & Ramos sp. nov., paratype (MNCN 15.05/63704), from a pond near Játar. **A**. Operculum, inner side. **B**. Operculum, outer side. **C**. Overview of radular teeth rows. **D–E**. Detailed view of the central and outer marginal teeth, respectively. **F**. Ctenidium and osphradium. **G**. Stomach. **H**. Partial nervous system. **I**. Pallial oviduct. **J**. Bursa copulatrix and seminal receptacle. **K**. Head of male and penis. Abbreviations: Ag = albumin gland; Bc = bursa copulatrix; Bd = bursal duct; Cg = capsule gland; Ct = ctenidium; Os = osphradium; Ro = renal oviduct; Sr = seminal receptacle.

Ecology and distribution

The species is restricted to a single spring and two connected ponds in the Granada Province, southern Spain. Specimens were found on submerged stones. Co-occurring gastropod species included *Ancylus fluviatilis* O.F. Müller, 1774 in the spring, with both *A. fluviatilis* and *Potamopyrgus antipodarum* (J.E. Gray, 1843) present in the ponds. The Gordo Spring was last visited in 2024 according to the *Catálogo de Manantiales y Fuentes de Andalucía* (www.conocetusfuentes.com) and remains in good ecological condition (J.M. Barea Azcón pers. com.), suggesting that *C. ballestae* sp. nov. likely faces no significant habitat threats.

Remarks

Corrosella ballestae sp. nov. is among the largest species within this group, comparable in size to *C. luisi*. It can be distinguished from other taxa in the same clade by its more tubular penis shape, a longer seminal receptacle (with most other species averaging under 0.30 mm in length, except for *C. luisi*, which has a similarly sized receptacle; Delicado *et al.* 2012), and the longest prostate gland recorded among species of *Corrosella*, mean length of approximately 2.20 mm. Although *C. ballestae* shares more morphological characteristics with *C. luisi*, it is phylogenetically closer to *C. andalusica* (Fig. 1), exhibiting an average sequence divergence of 7.1% from *C. luisi* and 7% from *C. andalusica* for the COI gene (Supp. file 1: Table S3).

Species of *Corrosella* from northern Iberia can be differentiated from *C. ballestae* sp. nov. by several traits: smaller shell size, a greater number of cusps on radular teeth, a cylindrical bursa copulatrix, a shorter seminal receptacle, a more triangular penis that is centrally positioned on the head, and a more strongly pigmented renal oviduct extending to the seminal receptacle.

Corrosella hinzi (Boeters, 1986)
Figs 6–7

Pseudamnicola (*Corrosella*) *hinzi* Boeters, 1986: 125, figs 1–3, pl. 18a fig. 1.

Pseudamnicola (*Corrosella*) *hinzi* – Boeters 1988: 205, figs 62, 72, 85, pl. 2 fig. 21 [partim; non figs 63–64, 73, 86]. — Boeters *et al.* 2015: 97.

Type material

Holotype

SPAIN • 1 spec. (sex unknown); Zaragoza, Bulbuente, Balsa de Vargas (at Borja according to Delicado *et al.* 2010: 101); SMF 257406; designated by Boeters (1986).

Paratypes

SPAIN • numerous specs; Zaragoza, Bulbuente; SMF 257407/5 • numerous specs; same data as for preceding; BOE 599, 600 and 1240.

Material examined

SPAIN – **Teruel Province** • 8 specs; spring of river park in Calamocha; 40.9261° N, 1.2989° W; 10 Dec. 2009; R.M. Álvarez-Halcón leg.; MNCN 15.05/63701 • 3 specs; Caminreal, Prado Spring; 40.8452° N, 1.3343° W; 10 Dec. 2009; R.M. Álvarez-Halcón leg.; MNCN 15.05/63702. – **Zaragoza Province** • 18 specs; Borja, Balsa de Vargas; 41.8253° N, 1.5525° W; 7 Oct. 2009; R.M. Álvarez-Halcón leg.; MNCN 15.05/63698 • 17 specs; Borja, Cazuelas Spring; 41.8225° N, 1.5502° W; 14 July 2009; R.M. Álvarez-Halcón leg.; MNCN 15.05/63699.

Description

Shell. Ovate-conic, whorls 4, height 2.75–3.50 mm (Fig. 6A–F); periostracum yellowish, strongly eroded, especially on early whorls; protoconch 1.5 whorls, diameter ca 425 µm, nucleus ca 150 µm wide (Fig. 6G); protoconch microsculpture pitted (Fig. 6H–I); teleoconch whorls convex, separated by deep sutures; peristome orthocline; inner lip thicker than outer lip, partially covering umbilicus; aperture margin slightly sinuate adapically (Fig. 6F).

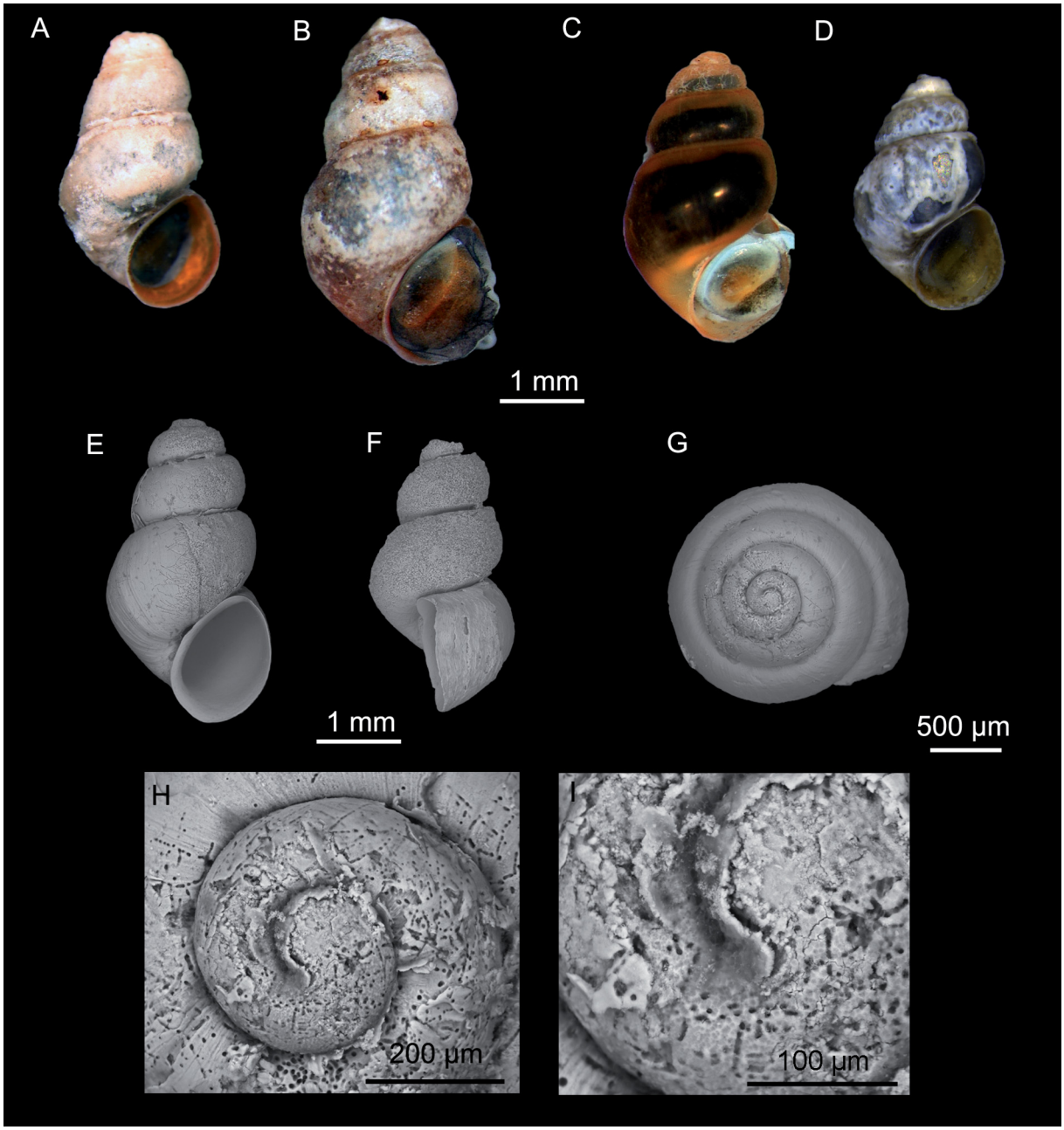

Fig. 6. Shells of *Corrosella hinzi* (Boeters, 1986). **A, E–I**. Balsa de Vargas, Borja, Zaragoza (MNCN 15.05/63698). **B**. Spring of river park in Calamocha, Teruel (MNCN 15.05/63701). **C**. Prado Spring, Caminreal, Teruel (MNCN 15.05/63702). **D**. Cazuelas Spring, Borja, Zaragoza (MNCN 15.05/63699). **A–E**. Frontal views. **F**. Lateral view. **G–H**. Details of the protoconch. **I**. Protoconch microsculpture.

Operculum. Corneous, yellowish, thin, pliable, ellipsoidal, paucispiral with submarginal nucleus, 2.75 whorls; muscle attachment oval, located near nucleus (Fig. 7A–B).

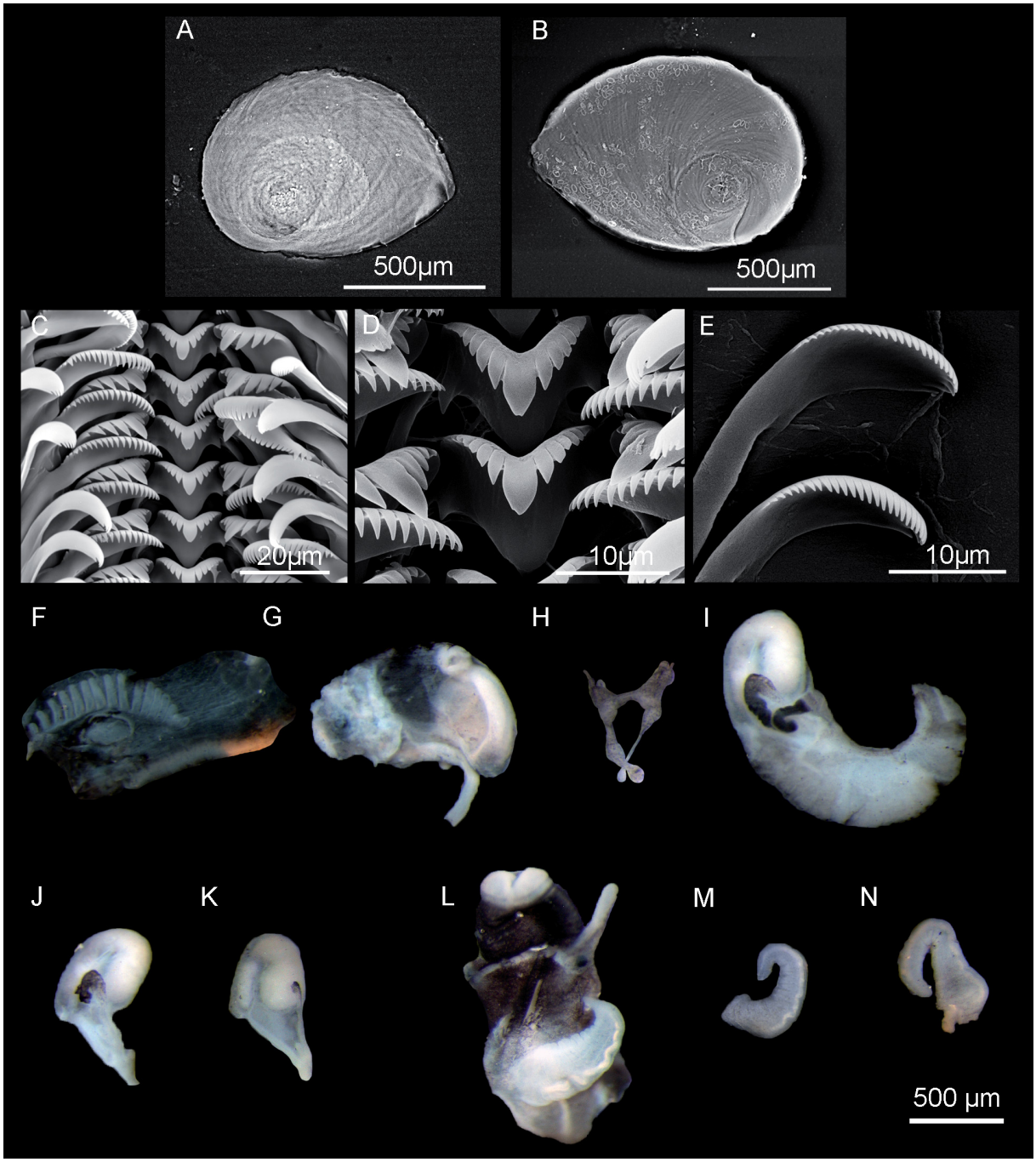

Fig. 7. Anatomy of *Corrosella hinzi* (Boeters, 1986). **A–J, L**. Balsa de Vargas, Borja, Zaragoza (MNCN 15.05/63698). **K, N**. Spring of river park in Calamocha, Teruel (MNCN 15.05/63701). **M**. Cazuelas Spring, Borja, Zaragoza (MNCN 15.05/63699). **A**. Operculum, inner side. **B**. Operculum, outer side. **C**. Overview of radular teeth rows. **D–E**. Detailed views of the central and outer marginal teeth, respectively. **F**. Ctenidium and osphradium. **G**. Stomach. **H**. Partial nervous system. **I**. Pallial oviduct. **J–K**. Bursa copulatrix and seminal receptacle. **L**. Head of male and penis. **M–N**. Penises.

Radula. Length intermediate (20% of total shell length), approximately 8 times as long as wide; having ca 65 rows of teeth. Central tooth formula 6-C-6/1-1, central cusp V-shaped, cutting edge slightly concave (Fig. 7C–D). Lateral tooth formula 4-C-4, central cusp V-shaped, slightly shorter than that central tooth. Inner marginal teeth with 22–24 cusps; outer marginal teeth with 27–29 cusps (Fig. 7E).

Pigmentation and anatomy. Head dark brown, pigmented from snout to neck (Fig. 7L); lighter pigmentation on neck and tip of the snout; tentacles with medial brown stripe; ocular lobes unpigmented; snout as long as wide, with a strong distal lobation; foot intermediate in length, pigmented dorsally. Ctenidium located anterior in pallial cavity; 14–18 gill filaments, taller than wide. Osphradium intermediate in width, positioned opposite middle of ctenidium (Fig. 7F). Stomach slightly longer than wide; posterior chamber slightly larger than anterior chamber (Fig. 7G); large gastric caecum; style sac longer than wide, encircled by intestine with a small patch of brown pigment.

Nervous system. Dark brown pigmentation, elongated (mean RPG ratio = 0.58); cerebral ganglia equal in size, darker than other ganglia and connectives; supraoesophageal connective ca 6 times as long as pleurosuboesophageal one (Fig. 7H).

Female genitalia. Capsule gland one-third longer than albumen gland (Fig. 7I); bursa copulatrix pyriform to elongate, folded in U-shaped; bursal duct slightly shorter than bursa; renal oviduct coiled, with 2–3 loops, pigmented to last loop; seminal receptacle pyriform with short duct, positioned slightly above junction of bursal duct and renal oviduct (Fig. 7J–K).

Male genitalia. Prostate gland about 3 times as long as wide. Penis gradually tapering, slightly pigmented centrally, with folds along inner edge, attached to the central area of head (Fig. 7L–N).

Ecology and distribution

The species has been recorded from four spring systems in the Zaragoza and Teruel provinces, north-east Spain. These springs are characterised by clean, well-oxygenated water with low temperatures (15–19°C), conductivity below 1 mS/cm² and a continuous but moderate flow. Specimens occur in high densities on stones, rocks, sandy or gravelly substrates and the submerged parts of aquatic vegetation. *Potamopyrgus antipodarum* was found co-occurring at all localities except in the River Park Spring in Calamocha, where the species was found alongside *Theodoxus* sp.

Remarks

Molecular and morphological studies (Delicado *et al.* 2013; Boeters *et al.* 2015), based on specimens collected from the type locality, indicate that *C. hinzi* does not occur in Pozo Azul (Burgos Province) as previously declared by Boeters (1988). Instead, our study revealed that this population, along with those from nearby areas, belongs to *C. navasiana*, thereby restricting the distribution of *C. hinzi* to a few localities in the northeastern Iberian Peninsula. Despite its limited range, anatomical differences exist within *C. hinzi*: populations from Teruel Province exhibit longer shells and penises (Fig. 7M–N) compared to those from Zaragoza Province, although they share similar female genitalia, nervous systems, and stomach structures.

Corrosella navasiana (Fagot, 1907)
Figs 8–11

Amnicola navasiana Fagot, 1907: 158, type locality “Bulbuente (Navás)”.
Pseudamnicola (*Corrosella*) *collingi* Boeters, Callot-Girardi & Knebelsberger, 2015: 98, figs 3, 12–13, 27–29, 41, 46, 53–55, table 1. **Syn. nov.**

Pseudamnicola (*Corrosella*) *valladolensis valladolensis* Boeters, Callot-Girardi & Knebelsberger, 2015: 103, figs 4–6, 14–17, 30–33, 42, 47, 56–57. **Syn. nov.**
Pseudamnicola (*Corrosella*) *tajoensis* Boeters, Callot-Girardi & Knebelsberger, 2015: 106, figs 9, 20–23, 38–39, 44, 49, 61–64. **Syn. nov.**
Pseudamnicola (*Corrosella*) *segoviana* Talaván-Serna & Talaván-Gómez, 2019: 3. **Syn. nov.**

Pseudamnicola navasiana – Vidal-Abarca & Suárez 1985: 18.
Pseudamnicola (*Corrosella*) *navasiana* – Boeters 1988: 203, figs 65, 71, 87, pl. 2: fig. 20. — Boeters *et al.* 2015: 111.

Type material

Unknown.

Type locality

Spain, Zaragoza, Bulbuente.

Material examined

SPAIN – **Burgos Province** • 16 specs; Covanera, Pozo Azul Spring; 42.7396° N, 3.7976° W; 1 May 2008; D. Delicado leg.; MNCN 15.05/63675 • 11 specs; a stream in Tubilleja; 42.8535° N, 3.7149° W; 3 May 2008; D. Delicado leg.; MNCN 15.05/63677 • 11 specs; Tubilla del Agua, La Toba Spring; 42.7087° N, 3.8046° W; 1 May 2008; D. Delicado leg.; MNCN 15.05/63673 • 1 spec.; Sedano, Valdeménez Stream; 42.7163° N, 3.8007° W; 1 May 2008; D. Delicado leg.; MNCN 15.05/63679 • 15 specs; a stream in Valtubilla; 42.7268° N, 3.7529° W; 1 May 2008; D. Delicado leg.; MNCN 15.05/63678. – **Cuenca Province** • 22 specs; El Hosquillo, Tía Perra Spring; 40.3709° N, 2.0054° W; 9 Mar. 2008; D. Delicado leg.; MNCN 15.05/63695. – **Guadalajara Province** • 11 specs; Somolinos, Canalejas Spring; 41.2577° N, 3.0710° W; 5 Apr. 2008; D. Delicado leg.; MNCN 15.05/63660 • 11 specs; Somolinos, Manadero River; 41.2570° N, 3.0741° W; 5 Apr. 2008; D. Delicado leg.; MNCN 15.05/63654 • 10 specs; Cabrera, Dulce River; 41.0077° N, 2.6763° W; 6 Apr. 2008; D. Delicado leg.; MNCN 15.05/63656 • 16 specs; a spring in Peralejos de las Truchas; 40.6113° N, 1.9615° W; 6 Apr. 2008; D. Delicado leg.; MNCN 15.05/63653. – **Segovia Province** • 32 specs; a spring next to the Sanctuary Virgen de la Fuencisla; 40.9562° N, 4.1319° W; 6 Jul. 2019; J.P. Miller and M. Carrillo leg.; MNCN 15.05/97257. – **Soria Province** • 11 specs; Medinaceli, Tinte Spring; 41.1592° N, 2.4271° W; 25 May 2010; R.M. Álvarez-Halcón leg.; MNCN 15.05/63643 • 17 specs; a spring in Arbujuelo; 41.1361° N, 2.3790° W; 25 May 2010; R.M. Álvarez-Halcón leg.; MNCN 15.05/63625. – **Toledo Province** • 18 specs; Ontígola, María Spring; 39.9979° N, 3.5774° W; 21 Oct. 2007; D. Delicado leg.; MNCN 15.05/63670 • 28 specs; a ditch in Borox; 40.0571° N, 3.7388° W; 9 Jun. 2007; D. Delicado leg.; MNCN 15.05/63668. – **Valladolid Province** • 10 specs; Quintanilla de Onésimo, Aceña Spring; 41.6279° N, 4.3623° W; 3 Sep. 2016; J.P. Miller and M. Carrillo leg.; MNCN 15.05/97200. – **Zaragoza Province** • 33 specs; Bulbuente, Fonnueva Spring; 41.8183° N, 1.3873° W; 1 May 2007; D. Delicado and R.M. Álvarez-Halcón leg.; MNCN 15.05/53718 • 16 specs; Ojos de Cimballa Wetland; 41.6381° N, 1.2876° W; 24 Feb. 2005; R.M. Álvarez-Halcón leg.; MNCN 15.05/63617 • 1 spec.; a spring in Mesones; 41.5517° N, 1.5362° W; 10 Feb. 2009; R.M. Álvarez-Halcón leg.; MNCN 15.05/63635 • 13 specs; Navalos, Espejo Lake; 41.1975° N, 1.7881° W; 27 May 2010; R.M. Álvarez-Halcón leg.; MNCN 15.05/63624.

Description

Shell. Ovate-conic, whorls 4, height 2.50–4.50 mm (Fig. 8); periostracum greyish or yellowish, often eroded, especially on early whorls; protoconch with 1.5 whorls, diameter ca 425 µm, nucleus ca 125 µm wide (Fig. 9A); protoconch microsculpture grooved or pitted (Fig. 9B–C); teleoconch whorls convex,

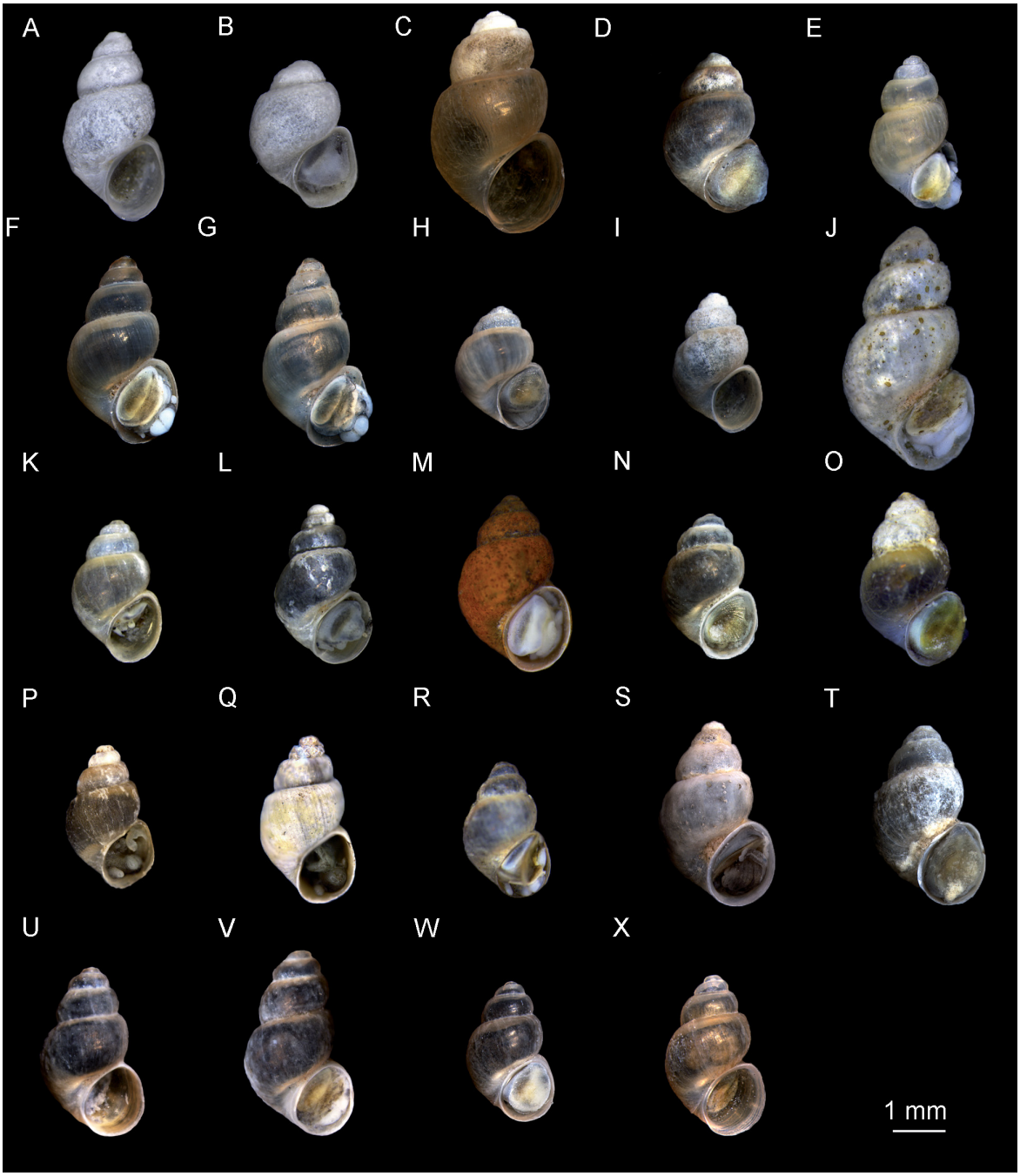

Fig. 8. Shells of *Corrosella navasiana* (Fagot, 1907). **A–B**. Fonnueva Spring, Bulbuente, Zaragoza (MNCN 15.05/53718). **C–D**. Ojos de Cimballa Wetland, Zaragoza (MNCN 15.05/63617). **E**. A spring in Arbujuelo, Soria (MNCN 15.05/63625). **F–G**. Tinte Spring, Medinaceli, Soria (MNCN 15.05/63643). **H–I**. Manadero River, Guadalajara (MNCN 15.05/63654). **J**. Tía Perra Spring, El Hosquillo, Cuenca (MNCN 15.05/63695). **K–L**. Pozo Azul Spring, Covanera, Burgos (MNCN 15.05/63675). **M**. A stream in Tubilleja, Burgos (MNCN 15.05/63677). **N**. La Toba Spring, Tubilla del Agua, Burgos (MNCN 15.05/63673). **O**. A stream in Valtubilla, Burgos (MNCN 15.05/63678). **P–Q**. María Spring, Ontígola, Toledo (MNCN 15.05/63670). **R**. A ditch in Borox, Toledo (MNCN 15.05/63668). **S–T**. A spring in Peralejos de las Truchas, Guadalajara (MNCN 15.05/63653). **U–V**. A spring next to the Sanctuary Virgen de la Fuencisla, Segovia (MNCN 15.05/97257). **W–X**. Aceña Spring, Quintanilla de Onésimo, Valladolid (MNCN 15.05/97200).

separated by deep sutures; last body whorl about ⅔ of total length; peristome orthocline; inner lip thicker than outer lip, partially hiding umbilicus; aperture margin simple, straight.

Operculum. Corneous, yellowish, thin, pliable, ellipsoidal, paucispiral with submarginal nucleus, 2.75 whorls; muscle attachment oval, located near nucleus.

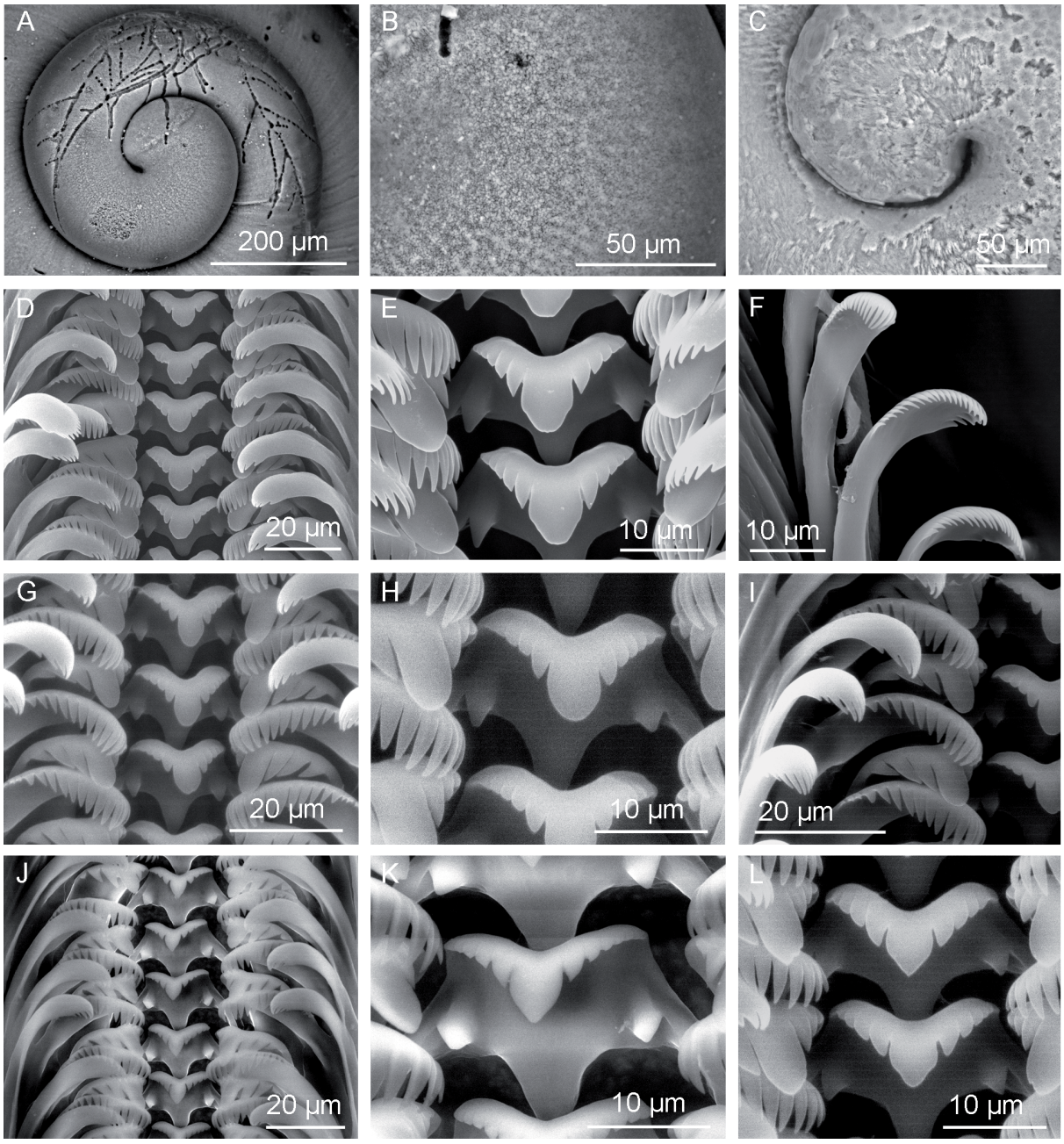

Fig. 9. Protoconch and radula of *Corrosella navasiana* (Fagot, 1907). **A–B, D–F**. Fonnueva Spring, Bulbuente, Zaragoza (MNCN 15.05/53718). **C, G–I**. Pozo Azul Spring, Covanera, Burgos (MNCN 15.05/63675). **J–K**. María Spring, Ontígola, Toledo (MNCN 15.05/63670). **L**. Tía Perra Spring, El Hosquillo, Cuenca (MNCN 15.05/63695). **A**. Details of the protoconch. **B–C**. Protoconch microsculpture. **D–L**. Overview of radular teeth rows and detailed view of the central, lateral and marginal teeth.

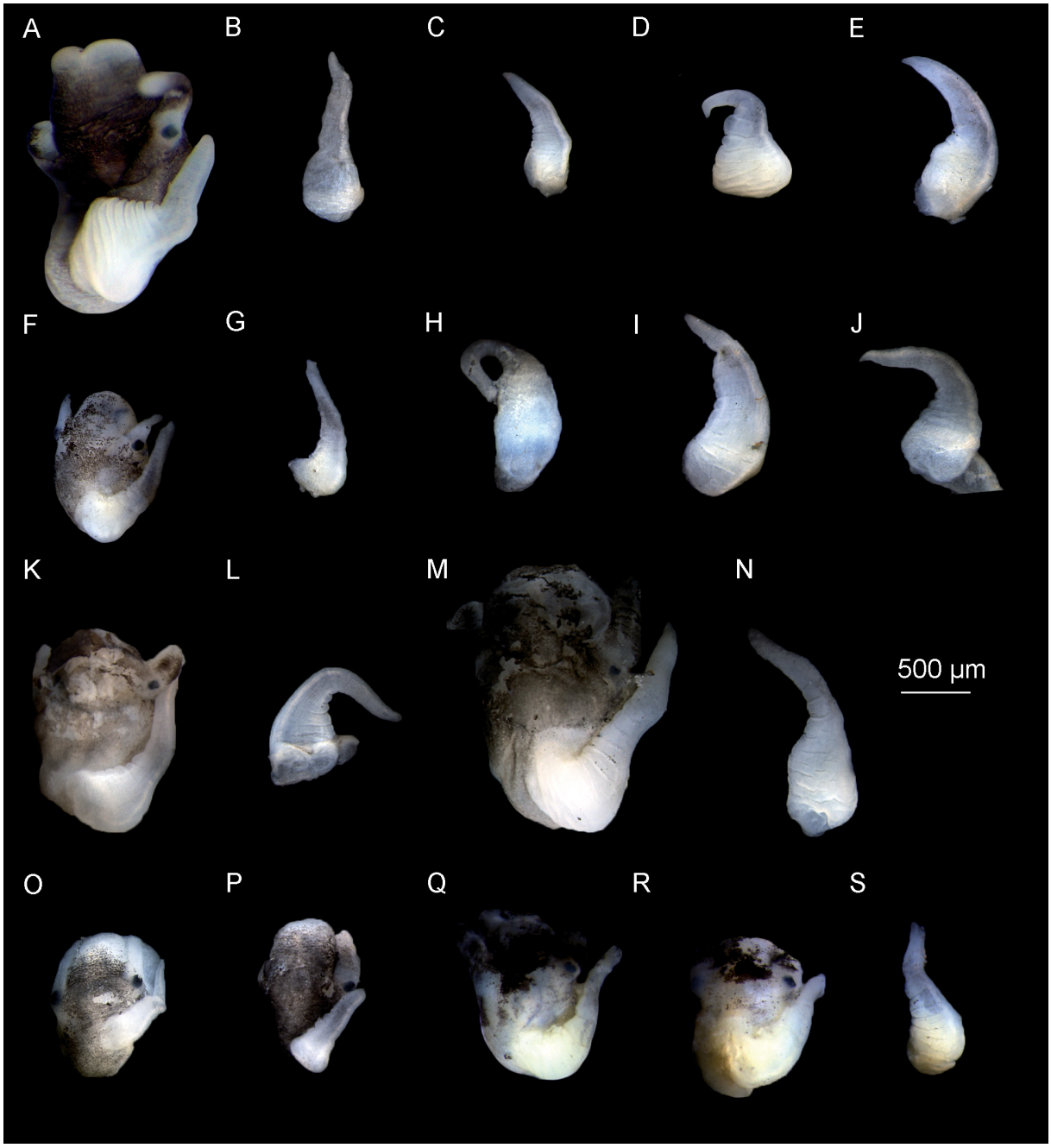

Fig. 10. Heads and penises of *Corrosella navasiana* (Fagot, 1907). **A**. Fonnueva Spring, Bulbuente, Zaragoza (MNCN 15.05/53718). **B**. Ojos de Cimballa Wetland, Zaragoza (MNCN 15.05/53717). **C**. A spring in Arbujuelo, Soria (MNCN 15.05/63625). **D**. Tinte Spring, Medinaceli, Soria (MNCN 15.05/63643). **E**. Tía Perra Spring, El Hosquillo, Cuenca (MNCN 15.05/63695). **F–H**. Pozo Azul Spring, Covanera, Burgos (MNCN 15.05/63675). **I**. La Toba Spring, Tubilla del Agua, Burgos (MNCN 15.05/63673). **J**. A stream in Valtubilla, Burgos (MNCN 15.05/63678). **K–L**. A ditch in Borox, Toledo (MNCN 15.05/63668). **M–N**. A spring in Peralejos de las Truchas, Guadalajara (MNCN 15.05/63653). **O–P**. Aceña Spring, Quintanilla de Onésimo, Valladolid (MNCN 15.05/97200). **Q–S**. A spring next to the Sanctuary Virgen de la Fuencisla, Segovia (MNCN 15.05/97257). All penises are shown in dorsal view except L, which is presented in ventral view.

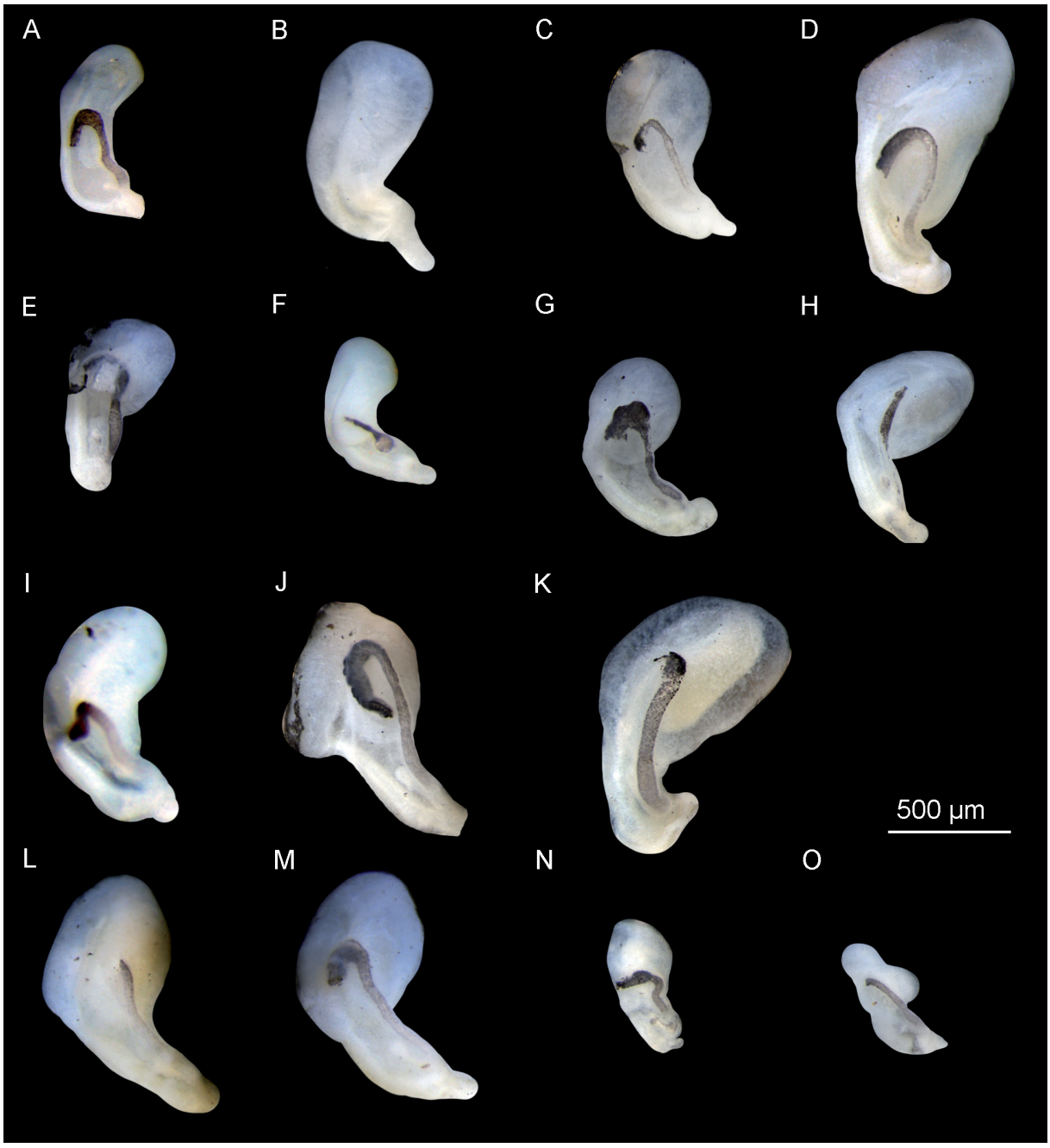

Fig. 11. Distal female genitalia of *Corrosella navasiana* (Fagot, 1907). **A**. Fonnueva Spring, Bulbuente, Zaragoza (MNCN 15.05/53718). **B**. Dulce River, Cabrera, Guadalajara (MNCN 15.05/63656). **C**. Canalejas Spring, Somolinos, Guadalajara (MNCN 15.05/63660). **D**. Tía Perra Spring, El Hosquillo, Cuenca (MNCN 15.05/63695). **E–F**. Pozo Azul Spring, Covanera, Burgos (MNCN 15.05/63675). **G**. La Toba Spring, Tubilla del Agua, Burgos (MNCN 15.05/63673). **H**. A stream in Valtubilla, Burgos (MNCN 15.05/63678). **I**. A ditch in Borox, Toledo (MNCN 15.05/63668). **J–K**. A spring in Peralejos de las Truchas, Guadalajara (MNCN 15.05/63653). **L–M**. A spring next to the Sanctuary Virgen de la Fuencisla, Segovia (MNCN 15.05/97257). **N–O**. Aceña Spring, Quintanilla de Onésimo, Valladolid (MNCN 15.05/97200).

Radula. Length intermediate (25% of shell length), approximately 8 times as long as wide; having ca 55 rows of teeth. Central tooth formula 4-C-4/1-1, central cusp U- or V-shaped (Fig. 9D–E, G–H, J–K), cutting edge slightly concave. Lateral tooth formula (3)4-C-4(3), central cusp U-shaped. Inner marginal teeth with 18–22 cusps; outer marginal teeth with 20–24 cusps (Fig. 9F, I, L).

Pigmentation and anatomy. Head dark brown, pigmented from snout to neck (Fig. 10A, F, K, M, O–R); lighter pigmentation on neck; tentacles with central brown stripe; ocular lobes unpigmented; snout as long as wide, with pronounced distal lobation; foot intermediate in length, dorsally pigmented. Ctenidium located anterior in pallial cavity; 15–20 gill filaments, taller than wide. Osphradium intermediate in width, positioned opposite middle of ctenidium. Stomach slightly longer than wide; posterior chamber slightly larger than anterior; style sac longer than wide, surrounded by intestine with small brown patch.

Nervous system. Dark brown pigmentation, moderately concentrated (mean RPG ratio = 0.48); cerebral ganglia equal in size and darker than other ganglia and connectives; supraoesophageal connective ca 6 times as long as pleurosuboesophageal one.

Male genitalia. Prostate gland about 3 times as long as wide. Penis gradually tapering, slightly pigmented centrally, with folds along inner edge; attached at central head area; penial duct straight or undulating along outer side of penis (Fig. 10).

Female genitalia. Capsule gland longer than albumen gland; bursa copulatrix pyriform to elongate, U-shaped fold; bursal duct shorter than bursa, partly or fully embedded in bursa copulatrix; renal oviduct coiled, with 2–3 loops, pigmented up to bursal duct insertion; seminal receptacle small, pyriform, with short duct, positioned slightly above junction of bursal duct and renal oviduct; seminal receptacle and bursa copulatrix broadly separated, occasionally nearly touching (Fig. 11).

Ecology and distribution

The species is widely distributed across the Ebro, Tajo and Duero River basins in central and northeastern Spain. It inhabits springs and streams with clean, well-oxygenated waters and typically abundant vegetation. Populations are often found in high densities, with specimens attached to stones and submerged vegetation. The species co-occurs with several other gastropods, including *Alzoniella cantabrica* (Boeters, 1983), *Spathogyna fezi* Arconada & Ramos, 2002, *Galba truncatula* (O.F. Müller, 1774), *Potamopyrgus antipodarum* and *Theodoxus* sp.

Remarks

Delicado *et al.* (2013) identified three subclades within *Corrosella navasiana*: one including populations from Burgos, Cuenca, Guadalajara, Soria and Zaragoza (with the type locality near Bulbuente, Zaragoza), a second from Burgos and a third from Toledo. Later, Boeters *et al.* (2015) reinterpreted these molecular clades as representing distinct species, assigning the first to *C. navasiana* s. str., the Burgos clade to *C. collingi*, and the Toledo clade to *C. tajoensis*. Boeters *et al.* (2015) noted that specimens from the type locality of *C. navasiana* (i.e., Fonnueva Spring near Bulbuente, Zaragoza) differ from those of *C. collingi*, *C. tajoensis* and *C. valladolensis* in several diagnostic traits: deeper sutures between shell whorls, a shoulder on the body whorl, a separate bursal duct from the bursa copulatrix, absence of contact between the seminal receptacle and bursa and a straight penial duct. These features were proposed as distinguishing characteristics for *C. navasiana* relative to the other species of Clade 1 (Boeters *et al.* 2015). However, these traits are inconsistently observed in other populations from Burgos, Cuenca, Guadalajara, Soria and Zaragoza, which were recognised as part of the *C. navasiana* clade by Boeters *et al.* (2015: 111). Our geometric morphometric analysis revealed no significant differences in suture depth or whorl edge shapes among members of Clade 1 (Fig. 2A). Additionally, variations in the degree of bursal duct embedding were noted, with specimens from Fonnueva and Tía Perra Springs showing

complete embedding within the bursa copulatrix (Fig. 11A, D) and those from the Dulce River displaying partial embedding (Fig. 11B–C). The distance between the seminal receptacle and the bursa –a non-influential trait in the CVA of female genitalia– and the outer edge undulation of the penial duct vary among *C. navasiana* populations (Figs 10A–E, 11A–D) and may also vary in *C. collingi* (Figs 10F–J, 11E–H). While these traits may appear to distinguish the species of Clade 1 when only the *C. navasiana* specimens from the type locality are considered (Boeters *et al.* 2015), they do not hold when individuals from the entire range are examined. The expanded morphospace of *C. navasiana* encompasses all species of Clade 1 described by Boeters *et al.* (2015). Furthermore, molecular delimitation methods did not distinguish these populations as separate taxa. Thus, all analysed populations are best interpreted as belonging to a single, morphologically variable species, *C. navasiana*, which is widely distributed across the Ebro, Tajo and Duero River basins in central and northeastern Iberia and exhibits notable morphological variation within and between subclades.

Discussion

This study evaluated the taxonomic status of 24 recognised species of *Corrosella*, integrating an expanded multilocus molecular dataset with morphology and geographic distribution data for 22 of these taxa and presenting shell measurements for the remaining two species known only from empty shells. Molecular species delimitation methods generally agreed on most groups, consistently validating two-thirds of the studied taxa (Fig. 1). Based on these results, along with geographic isolation and CVA validation, groups delimited by ASAP within Clades 2, 4 and 5 – most of which were corroborated by GMYC and PTP – are recognised as 12 valid species. These correspond to species described from southern Iberia and the Maghreb (Delicado *et al.* 2012, 2013; Boulaassafer *et al.* 2021). However, certain clades, particularly underrepresented ones with high DNA sequence diversity and complex phylogenetic structure (e.g., Clade 3), may be oversplit by molecular delimitation methods. Thus, we recognise two putative species within Clade 3 instead of the delimited four groups. Species in Clade 3, along with the single species in Clade 6, exhibit cryptic characteristics due to overlapping shell and male genital traits despite notable DNA sequence divergence, a pattern also noted by Delicado *et al.* (2012) for species in Clade 3, consistent with trends observed in other hydrobiid groups (Liu *et al.* 2003; Hofman *et al.* 2022; Miller *et al.* 2023).

Expanding the datasets for Clade 1 revealed greater overlap in morphological variation among populations of the closely related species within this clade (Boeters *et al.* 2015), with *C. navasiana* exhibiting notable morphological variation and occupying a morphospace that encompasses the entire clade, including all species previously proposed by Boeters *et al*. (2015). This overlap has blurred species boundaries to the extent that these populations are best considered as a single species. Molecular, morphological and ecological data from topotype specimens (or near topotypes) did not support the separation of *C. navasiana*, *C. collingi*, *C. tajoensis*, *C. segoviana* and *C. valladolensis valladolensis* as distinct species (Figs 1–2). We therefore propose synonymising these taxa under the earliest available name, *C. navasiana*. This finding aligns with Boeters *et al.* (2015), who noted that COI sequence divergence did not distinguish *C. collingi*, *C. tajoensis*, and *C. navasiana*, an outcome also supported by our ASAP analysis and by species delimitation methods (GMYC and PTP) applied to mitochondrial COI and 16S markers. Although many hydrobiid species described in recent decades exhibit DNA divergence and reciprocal monophyly, exceptions arise where morphological distinctions occur among closely related species, as observed in species of *Pseudamnicola* from Majorca (Delicado *et al.* 2025). The morphological differences seen in individuals from the type localities (or adjacent regions) of *C. collingi*, *C. tajoensis*, *C. v. valladolensis* and *C. navasiana* (Boeters *et al.* 2015) are thus not supported as species-level distinctions upon examination of additional populations (see *C. navasiana* in the Systematics section). Our CVA analysis, incorporating data from more populations, showed that shell and genitalia features did not discriminate species within Clade 1. We acknowledge that the number of individuals

dissected for genitalia analyses was limited due to specimen availability and preservation constraints; however, additional data would not eliminate the observed overlap, which likely reflects genuine morphological conservatism rather than methodological bias. Additionally, *C. segoviana*, initially differentiated solely by penis dimensions from *C. valladolensis* (Talaván-Serna & Talaván-Gómez 2019), showed no separation in our genitalia analyses (Fig. 2D). Sequencing topotypical specimens of *C. segoviana* for the first time revealed a lack of monophyly and minimal DNA sequence divergence from *C. valladolensis* and *C. navasiana*, further supporting its synonymisation with *C. navasiana*.

Reassessment of outlier species, such as *Corrosella hydrobiopsis*, also aids in refining genus-level taxonomy. This species, originally described from three empty shells (Boeters 1999) and for which we have only shell measurements, fell entirely outside the *Corrosella* morphospace in shell size and shape analyses, suggesting it may not belong to the genus (Fig. 2). Its turriform shell shape contrasts with the ovate-conic shells typical of *Corrosella*, and its tall, less convex spire whorls align more with Moitessieriidae Bourguignat, 1863 snails (Boeters 2003; Boeters *et al.* 2013). However, in the absence of anatomical or molecular data, this resemblance remains tentative, and the taxonomic placement of *C. hydrobiopsis* within Moitessieriidae cannot be confirmed. Until new material becomes available for detailed examination, the species should be provisionally retained within *Corrosella*, albeit as an uncertain member of the genus. *Corrosella tejedoi*, on the other hand, classified originally based on shell morphology (Boeters *et al.* 2015), fell within the *Corrosella* morphospace in our analyses, suggesting its classification is likely correct. However, molecular data would substantiate its taxonomic certainty.

Ecologically, species of *Corrosella* display minimal differentiation, with shared habitat preferences across topography, hydroclimate and soil characteristics, suggesting these environmental factors do not serve as taxonomic discriminators – an observation common to other spring snails (Wilke *et al.* 2010). Most species inhabit upstream environments with cool temperatures (9°C–16°C), stable flow, near-neutral pH (6.5–7.4) and low to moderate soil organic carbon (10–40 g/kg). Nonetheless, variations in flow conditions were detected for four species (Fig. 3), indicating a broader tolerance to hydrological variability. The most widespread species in the genus, *C. navasiana*, occupies the broadest flow conditions, underscoring its ability to cope with diverse hydrological settings, either through local adaptation or inherently high tolerance. However, ecological data for *C. navasiana* from the most separated populations in the PCA – Tubilleja Stream and Aceña Spring – should be interpreted cautiously. The snails are found in smaller water flows parallel to the main basins of the Duero and Ebro Rivers and not directly in the basins, where GIS-derived habitat variables were available. Despite these exceptions, the narrow ecological tolerances of most species of *Corrosella* suggest an increased vulnerability to changes in water conditions, compounded by anthropogenic impacts such as water extraction and climate change (Álvarez-Halcón *et al.* 2012; Boulaassafer *et al.* 2023). Although aquatic vegetation can play a key role in shaping spring microhabitats and influencing physicochemical conditions, such data were unavailable for most sites. The absence of these records reflects heterogeneous sampling and the lack of high-resolution vegetation data at the spring scale, which limits ecological interpretation but does not affect the consistency of the abiotic analyses performed.

Our taxonomic revisions hold significant implications for conservation prioritisation within the genus. Our findings reveal that *C. navasiana* (currently listed as data deficient by the IUCN) has a broader distribution and wider ecological range than previously recognised (Boeters *et al.* 2015), indicating it may be of lower conservation priority. Species in southern and eastern Iberia are more widely distributed and include populations that have not yet been analysed genetically (Delicado & Ramos 2012; Delicado *et al.* 2012). Further research should incorporate these populations into molecular datasets to evaluate population dynamics, connectivity and migration rates, which are essential for accurate conservation assessment. *Corrosella ballestae* sp. nov. is known from a single locality and exhibits a deep DNA sequence divergence from its sister species, underscoring its distinct evolutionary lineage. This limited

distribution, combined with its deep DNA sequence divergence, makes *C. ballestae* a species of conservation concern, as it is particularly vulnerable to habitat disturbance and environmental changes. *Corrosella nechadae* and *C. hinzi* represent ancient lineages with restricted distributions and specialised ecological needs, meriting conservation attention. While *C. nechadae* is currently listed as 'Endangered' by the IUCN, *C. hinzi* lacks formal assessment under these criteria, though it appears in a regional red list. The narrow ecological niches of species of *Corrosella*, particularly *C. nechadae* and *C. hinzi*, increase their susceptibility to habitat alteration and climate-related stressors. Similar endemic freshwater species face increased extinction risks due to limited distribution ranges and habitat specialisation (Dudgeon *et al*. 2006). Conservation efforts should therefore prioritise protecting stable upstream habitats to mitigate these risks.

Our findings in *Corrosella* exemplify the importance of a representative sample size of individuals and integrative taxonomic approaches, particularly within morphologically conserved groups such as the Hydrobiidae. Recognising cryptic diversity (as in the case of *C. ballestae* sp. nov.) and refining species boundaries through molecular evidence (e.g. synonymising all species of Clade 1 under *C. navasiana*) establishes a framework that could be applied to resolve similar taxonomic ambiguities in other hydrobiid taxa. This study provides a groundwork for guiding conservation strategies and future taxonomic revisions within *Corrosella*, improving our understanding and protection of these ecologically significant spring snails.

Acknowledgements

We gratefully acknowledge Miguel Carrillo Pacheco and Ramón M. Álvarez Halcón for their support during fieldwork and for collecting samples; José Miguel Barea Azcón (Agencia de Medio Ambiente y Agua de Andalucía, Spain) for sharing material and recent habitat information; the technicians, Laura Tormo and Martha Furió (Non-destructive Techniques Laboratory, MNCN-CSIC, Madrid, Spain) for their assistance with the ESEM photomicrographs; Javier de Andrés and Dolores Bragado (the Mollusc Collection of the MNCN-CSIC) for the loan of material; Anna Jazwinska Müller (Department of Biology, University of Fribourg, Switzerland) for optical facilities at the University of Fribourg, Switzerland. Computational resources were provided by the de.NBI Cloud within the German Network for Bioinformatics Infrastructure (de.NBI). Three anonymous reviewers provided constructive and useful comments on an earlier version of the manuscript. This research was funded by the Spanish Ministry of Economy and Competitiveness (MINECO) through the research project Fauna Ibérica [grant numbers CGL2014-53332-C5-1-P and PGC2018-095851- B-C61], the Horizon Europe – Work Programme 2023-2024 under the Marie Skłodowska-Curie grant agreement no 101149372 PROTECT (to DD), the Swiss National Science Foundation (grant no. PCEFP3_187012) (to TH) and the Spanish Ministry of Science, Innovation and Universities granting a fellowship contract PTA2023-023686-I (to JPM).

References

Akaike H. 1974. A new look at the statistical model identification. *IEEE Transactions on Automatic Control* 19 (6): 716–723. https://doi.org/10.1109/TAC.1974.1100705

Alcántara de la Fuente M. 2007. *Catálogo de Especies amenazadas en Aragón*. *Fauna*. Departamento de Medio Ambiente del Gobierno de Aragón. Huesca, Spain.

Álvarez-Halcón R.M.Á., Millán C.R., Torres A.P., Delicado D., Ramos M.A., Ortí A.M., Lapresta M.A.G. & Tomás A.C. 2012. Gasterópodos acuáticos en la cuenca del Jalón: hábitats y amenazas. *Naturaleza aragonesa* 29: 35–42.

Araujo R., Remón J.M., Moreno D. & Ramos M.A. 1995. Relaxing techniques for freshwater molluscs: trials for evaluation of different methods. *Malacologia* 36 (1): 29–41.

Barea-Azcón J.M., Ballesteros-Duperón E. & Moreno D. 2008. *Libro Rojo de los Invertebrados de Andalucía*. *Vol. I.* Consejería de Medio Ambiente, Junta de Andalucía, Sevilla, Spain.

Boeters H.D. 1970. *Corrosella* n. gen. (Prosobranchia: Hydrobiidae). *Journal de Conchyliologie* 108 (3): 63–69.

Boeters H.D. 1984. Unbekannte westeuropäische Prosobranchia, 6. *Heldia* 1 (1): 9–11.

Boeters H.D. 1986. Unbekannte westeuropäische Prosobranchia, 7. *Heldia* 1: 125–128.

Boeters H.D. 1988. Moitessieriidae und Hydrobiidae in Spanien und Portugal. *Archiv für Molluskenkunde* 118: 181–261.

Boeters H.D. 1999. *Alzoniella navarrensis* n. sp., *Pseudamnicola* (*Corrosella*) *hydrobiopsis* n. sp. and the type species of *Pseudamnicola* Paulucci, 1878. Unknown west European Prosobranchia, 9. *Basteria* 63 (1/3): 77–81.

Boeters H.D. 2003. Supplementary notes on Moitessieriidae and Hydrobiidae from the Iberian Peninsula (Gastropoda: Caenogastropoda). *Basteria* 67: 1–41.

Boeters H.D., Glöer P. & Pešić V. 2013. Some new freshwater gastropods from southern Europe (Mollusca: Gastropoda: Truncatelloidea). *Folia Malacologica* 21 (4): 225–235. https://doi.org/10.12657/folmal.021.025

Boeters H.D., Callot-Girardi H. & Knebelsberger T. 2015. News of *Pseudamnicola* (*Corrosella*) of Spain and France (Mollusca: Gastropoda: Truncatelloidea). *Folia Malacologica* 23 (2): 95–119. https://doi.org/10.12657/folmal.023.007

Bouckaert R.R. & Drummond A.J. 2017. bModelTest: Bayesian phylogenetic site model averaging and model comparison. *BMC Evolutionary Biology* 17 (1): 42. https://doi.org/10.1186/s12862-017-0890-6

Bouckaert R., Vaughan T.G., Barido-Sottani J., Duchêne S., Fourment M., Gavryushkina A., Heled J., Jones G., Kühnert D., Maio N.D., Matschiner M., Mendes F.K., Müller N.F., Ogilvie H.A., Plessis L. du, Popinga A., Rambaut A., Rasmussen D., Siveroni I., … & Drummond A.J. 2019. BEAST 2.5: An advanced software platform for Bayesian evolutionary analysis. *PLoS Computational Biology* 15 (4): e1006650. https://doi.org/10.1371/journal.pcbi.1006650

Boulaassafer K., Ghamizi M., Machordom A., Albrecht C. & Delicado D. 2021. Hidden species diversity of *Corrosella* Boeters, 1970 (Caenogastropoda: Truncatelloidea) in the Moroccan Atlas reveals the ancient biogeographic link between North Africa and Iberia. *Organisms Diversity & Evolution* 21 (2): 393–420. https://doi.org/10.1007/s13127-021-00490-3

Boulaassafer K., Seddon M. & Ghamizi M. 2023. Small and vulnerable – What can be done to protect freshwater Hydrobiidae in Morocco? *Tentacle* 31: 19–20.

Castresana J. 2000. Selection of conserved blocks from multiple alignments for their use in phylogenetic analysis. *Molecular Biology and Evolution* 17 (4): 540–552. https://doi.org/10.1093/oxfordjournals.molbev.a026334

Darriba D., Taboada G.L., Doallo R. & Posada D. 2012. jModelTest 2: more models, new heuristics and parallel computing. *Nature Methods* 9 (8): 772. https://doi.org/10.1038/nmeth.2109

Davis G.M., Kitikoon V. & Temcharoen P. 1976. Monograph on "*Lithoglyphosis*" *aperta*, the snail host of Mekong River schistosomiasis. *Malacologia* 15: 241–287.

Delicado D. & Ramos M.A. 2012. Morphological and molecular evidence for cryptic species of springsnails [genus *Pseudamnicola* (*Corrosella)* (Mollusca, Caenogastropoda, Hydrobiidae)]. *ZooKeys* 190: 55–79. https://doi.org/10.3897/zookeys.190.2555

Delicado D., Ramos M.-Á., Halcón R.M.Á., Millán C.R., Torres A.P. & Grijalbo R.P. 2010. Presencia del molusco dulceacuícola *Pseudamnicola* (*Corrosella*) *hinzi* Boeters 1986 (Gastropoda: Caenogastropoda: Hydrobiidae) en Calamocha y Caminreal (Teruel). *Xiloca* 38: 101–110.

Delicado D., Machordom A. & Ramos M.A. 2012. Underestimated diversity of hydrobiid snails. The case of *Pseudamnicola* (*Corrosella*) (Mollusca: Caenogastropoda: Hydrobiidae). *Journal of Natural History* 46 (1–2): 25–89. https://doi.org/10.1080/00222933.2011.623358

Delicado D., Machordom A. & Ramos M.A. 2013. Living on the mountains: Patterns and causes of diversification in the springsnail subgenus *Pseudamnicola* (*Corrosella*) (Mollusca: Caenogastropoda: Hydrobiidae). *Molecular Phylogenetics and Evolution* 68 (3): 387–397. https://doi.org/10.1016/j.ympev.2013.04.022

Delicado D., Machordom A. & Ramos M.A. 2015. Effects of habitat transition on the evolutionary patterns of the microgastropod genus *Pseudamnicola* (Mollusca, Hydrobiidae). *Zoologica Scripta* 44 (4): 403–417. https://doi.org/10.1111/zsc.12104

Delicado D., Hauffe T. & Wilke T. 2018. Ecological opportunity may facilitate diversification in Palearctic freshwater organisms: a case study on hydrobiid gastropods. *BMC Evolutionary Biology* 18 (1): 55. https://doi.org/10.1186/s12862-018-1169-2

Delicado D., Hauffe T. & Wilke T. 2024. Fifth mass extinction event triggered the diversification of the largest family of freshwater gastropods (Caenogastropoda: Truncatelloidea: Hydrobiidae). *Cladistics* 40 (1): 82–96. https://doi.org/10.1111/cla.12558

Delicado D., Boulaassafer K., Khalloufi N. & Hauffe T. 2025. A holistic perspective on species delimitation outperforms all methods based on single data types in freshwater gastropods (Caenogastropoda: Hydrobiidae: *Pseudamnicola*). *Zoological Journal of the Linnean Society* 203: zlae010. https://doi.org/10.1093/zoolinnean/zlae010

Domisch S., Amatulli G. & Jetz W. 2015. Near-global freshwater-specific environmental variables for biodiversity analyses in 1 km resolution. *Scientific Data* 2 (1): 150073. https://doi.org/10.1038/sdata.2015.73

Dudgeon D., Arthington A.H., Gessner M.O., Kawabata Z.-I., Knowler D.J., Lévêque C., Naiman R.J., Prieur-Richard A.-H., Soto D., Stiassny M.L.J. & Sullivan C.A. 2006. Freshwater biodiversity: importance, threats, status and conservation challenges. *Biological Reviews* 81 (2): 163–182. https://doi.org/10.1017/S1464793105006950

Fagot P. 1907. Contribution à la faune malacologique de la province de Aragon. *Boletín de la Sociedad aragonesa de Ciencias naturales* 6: 136–160.

Gasull L. 1981. Fauna malacológica terrestre y de agua dulce de la provincia de Castellón de la Plana. *Bolletí de la Societat d'Història Natural de les Balears* 25: 53–101.

Gernhard T. 2008. The conditioned reconstructed process. *Journal of Theoretical Biology* 253 (4): 769–778. https://doi.org/10.1016/j.jtbi.2008.04.005

Hammer O., Harper D.A.T. & Ryan P.D. 2001. PAST: Paleontological Statistics Software Package for Education and Data Analysis. *Palaeontologica Electronica* 4: 9.

Hengl T., Jesus J.M. de, MacMillan R.A., Batjes N.H., Heuvelink G.B.M., Ribeiro E., Samuel-Rosa A., Kempen B., Leenaars J.G.B., Walsh M.G. & Gonzalez M.R. 2014. SoilGrids1km — Global soil information based on automated mapping. *PLoS ONE* 9 (8): e105992. https://doi.org/10.1371/journal.pone.0105992

Hershler R. & Ponder W.F. 1998. A review of morphological characters of hydrobioid snails. *Smithsonian Contributions to Zoology* 600: 1–55. https://doi.org/10.5479/si.00810282.600

Hofman S., Grego J., Beran L., Jaszczyńska A., Osikowski A. & Falniowski A. 2022. *Kerkia* Radoman, 1978 (Caenogastropoda: Hydrobiidae): endemism, apparently morphostatic evolution and cryptic speciation. *Molluscan Research* 42 (4): 295–319. https://doi.org/10.1080/13235818.2022.2129943

IUCN 2024. The IUCN Red List of Threatened Species. Version 2024-2.
Available from https://www.iucnredlist.org/en [accessed 1 Nov. 2024].

Kapli P., Lutteropp S., Zhang J., Kobert K., Pavlidis P., Stamatakis A. & Flouri T. 2017. Multi-rate Poisson tree processes for single-locus species delimitation under maximum likelihood and Markov chain Monte Carlo. *Bioinformatics* 33 (11): 1630–1638. https://doi.org/10.1093/bioinformatics/btx025

Katoh K. & Standley D.M. 2013. MAFFT multiple sequence alignment software version 7: improvements in performance and usability. *Molecular Biology and Evolution* 30 (4): 772–780.
https://doi.org/10.1093/molbev/mst010

Klingenberg C.P. 2011. MorphoJ: an integrated software package for geometric morphometrics. *Molecular Ecology Resources* 11 (2): 353–357. https://doi.org/10.1111/j.1755-0998.2010.02924.x

Kozlov A.M., Darriba D., Flouri T., Morel B. & Stamatakis A. 2019. RAxML-NG: a fast, scalable and user-friendly tool for maximum likelihood phylogenetic inference. *Bioinformatics* 35 (21): 4453–4455.
https://doi.org/10.1093/bioinformatics/btz305

Lehner B., Verdin K.L. & Jarvis A. 2008. New global hydrography derived from spaceborne elevation data. *Eos, Transactions American Geophysical Union* 89 (10): 93–94.
https://doi.org/10.1029/2008EO100001

Liu H.-P., Hershler R. & Clift K. 2003. Mitochondrial DNA sequences reveal extensive cryptic diversity within a western American springsnail. *Molecular Ecology* 12 (10): 2771–2782.
https://doi.org/10.1046/j.1365-294X.2003.01949.x

Martín-Álvarez J.F., Glöer P., López-Soriano J., Raven H., Alonso Á., Sánchez O. & Quiñonero-Salgado S. 2024. A new Hydrobiidae species of the genus *Corrosella* Boeters, 1970 from Andalusia (S Iberian Peninsula). *Nemus* 14: 112–121.

Martínez-Ortí A. 2018. Taxonomic revision of *Neohoratia herreroi* Bech, 1993 (Gastropoda, Hydrobiidae). *Basteria* 82 (1–3): 38–42.

Miller J.P., Delicado D., García-Guerrero F. & Ramos M.A. 2022. Recurrent founder-event speciation across the Mediterranean likely shaped the species diversity and geographic distribution of the freshwater snail genus *Mercuria* Boeters, 1971 (Caenogastropoda: Hydrobiidae). *Molecular Phylogenetics and Evolution* 173: 107524. https://doi.org/10.1016/j.ympev.2022.107524

Miller J.P., Delicado D., García-Guerrero F., Khalloufi N. & Ramos M.A. 2023. Morphology and taxonomic assessment of eight genetic clades of *Mercuria* Boeters, 1971 (Caenogastropoda, Hydrobiidae), with the description of five new species. *European Journal of Taxonomy* 866: 1–63.
https://doi.org/10.5852/ejt.2023.866.2107

MolluscaBase eds. 2025. MolluscaBase. Available from http://www.molluscabase.org [accessed 20 Jan. 2025].

Paradis E. & Schliep K. 2019. ape 5.0: an environment for modern phylogenetics and evolutionary analyses in R. *Bioinformatics* 35 (3): 526–528. https://doi.org/10.1093/bioinformatics/bty633

Perez K.E. & Minton R.L. 2008. Practical applications for systematics and taxonomy in North American freshwater gastropod conservation. *Journal of the North American Benthological Society* 27 (2): 471–483. https://doi.org/10.1899/07-059.1

Pons J., Barraclough T.G., Gomez-Zurita J., Cardoso A., Duran D.P., Hazell S., Kamoun S., Sumlin W.D. & Vogler A.P. 2006. Sequence-based species delimitation for the DNA taxonomy of undescribed insects. *Systematic Biology* 55 (4): 595–609. https://doi.org/10.1080/10635150600852011

Puillandre N., Brouillet S. & Achaz G. 2021. ASAP: assemble species by automatic partitioning. *Molecular Ecology Resources* 21 (2): 609–620. https://doi.org/10.1111/1755-0998.13281

QGIS Development Team 2023. QGIS Geographic Information System. QGIS Association. Available from https://qgis.org [accessed 1 Nov. 2024].

R Core Team 2025. R: A Language and environment for statistical computing. Vienna, Austria. Availablew from http://www.R-project.org/ [accessed 1 Nov. 2024].

Rambaut A. 2016. FigTree 1.4.3, a graphical viewer of phylogenetic trees.
Available from https://tree.bio.ed.ac.uk/software/figtree/ [accessed 30 Jan. 2023].

Rambaut A., Drummond A.J., Xie D., Baele G. & Suchard M.A. 2018. Posterior summarization in Bayesian phylogenetics using Tracer 1.7. *Systematic Biology* 67 (5): 901–904.
https://doi.org/10.1093/sysbio/syy032

Ramos M.A., Arconada B., Moreno D. & Rolán E. 2000. A new genus and a new species of hydrobiid snail (Mollusca: Gastropoda: Hydrobiidae) from eastern Spain. *Malacologia* 42 (1–2): 75–101.

Reid N.M. 2014. bGMYC: a Bayesian MCMC implementation of the general mixed Yule-coalescent model for species delimitation. R package version 1.0.2.
Available from https://nreid.github.io/assets/bGMYC_instructions_14.03.12.txt [accessed 2 Feb. 2023].

Reid N.M. & Carstens B.C. 2012. Phylogenetic estimation error can decrease the accuracy of species delimitation: a Bayesian implementation of the general mixed Yule-coalescent model. *BMC Evolutionary Biology* 12 (1): 196. https://doi.org/10.1186/1471-2148-12-196

Rohlf F.J. 2021. tpsDig 2 version 2.32. Department of Ecology and Evolution and Anthropology, State University of New York at Stony Brook, New York.

Ronquist F., Teslenko M., Van Der Mark P., Ayres D.L., Darling A., Höhna S., Larget B., Liu L., Suchard M.A. & Huelsenbeck J.P. 2012. MrBayes 3.2: efficient Bayesian phylogenetic inference and model choice across a large model space. *Systematic Biology* 61 (3): 539–542.
https://doi.org/10.1093/sysbio/sys029

Sheets H.D. 2014. Integrated Morphometrics Package (IMP). Canisius College and State University of New York, Buffalo.

Stekhoven D.J. & Bühlmann P. 2012. MissForest—non-parametric missing value imputation for mixed-type data. *Bioinformatics* 28 (1): 112–118. https://doi.org/10.1093/bioinformatics/btr597

Talaván-Serna J. & Talaván-Gómez J. 2019. *Pseudoamnicola* (*Corrosella*) *segoviana* nov. sp. from Castilla-León (Spain). *Malacologia Mostra Mondiale* 103: 3–4.

Talaván-Serna J. & Talaván-Gómez J. 2024. *Corrosella arlanzonica* nov. sp. (Truncatelloidea: Hydrobiidae) from the Neogene of the Iberian Peninsula. *Malacologia Mostra Mondiale* 122: 17.

Tamura K., Stecher G. & Kumar S. 2021. MEGA11: Molecular Evolutionary Genetics Analysis Version 11. *Molecular Biology and Evolution* 38 (7): 3022–3027. https://doi.org/10.1093/molbev/msab120

Vidal-Abarca M.R. & Suárez M.L. 1985. *Lista faunística y bibliográfica de los Moluscos (Gastrópoda* [sic] *y Bivalvia) de las Aguas continentales de la Península Ibérica e Islas Baleares*. Asociación Española de Limnología; Universitat Barcelona Editions, Madrid, Spain.
Available from https://www.limnetica.com/es/otras-publicaciones [accessed 1 Nov. 2024].

Wilke T., Davis G.M., Qiu D.C. & Spear R.C. 2006. Extreme mitochondrial sequence diversity in the intermediate schistosomiasis host *Oncomelania hupensis robertsoni*: another case of ancestral polymorphism? *Malacologia* 48 (1–2): 143–157.

Wilke T., Benke M., Brändle M., Albrecht C. & Bichain J.-M. 2010. The neglected side of the coin: Non-adaptive radiations in spring snails (*Bythinella* spp.). *In*: Glaubrecht M. (ed.) *Evolution in Action*: 551–578. Springer, Berlin Heidelberg. https://doi.org/10.1007/978-3-642-12425-9_25

Zhang J., Kapli P., Pavlidis P. & Stamatakis A. 2013. A general species delimitation method with applications to phylogenetic placements. *Bioinformatics* 29 (22): 2869–2876. https://doi.org/10.1093/bioinformatics/btt499

Printed versions of all papers are deposited in the libraries of two of the institutes that are members of the *EJT* consortium: Muséum national d'Histoire naturelle, Paris, France and Royal Museum for Central Africa, Tervuren, Belgium. The other members of the consortium are: Royal Belgian Institute of Natural Sciences, Brussels, Belgium; Meise Botanic Garden, Meise, Belgium; Natural History Museum of Denmark, Copenhagen, Denmark; Naturalis Biodiversity Center, Leiden, the Netherlands; Museo Nacional de Ciencias Naturales-CSIC, Madrid, Spain; Leibniz Institute for the Analysis of Biodiversity Change, Bonn – Hamburg, Germany; National Museum of the Czech Republic, Prague, Czech Republic; The Steinhardt Museum of Natural History, Tel Aviv, Israël.

Supplementary files

Supp. file 1. Supporting information. https://doi.org/10.5852/ejt.2026.1043.3203.14217

Table S1. Species names, locality data, locality codes, number of shells used in the geometric morphometric analysis, number of dissected (Diss) and sequenced (#DNA) individuals and GenBank accession numbers for the *Corrosella* populations included in the molecular analyses.

Table S2. Quantitative variables (and abbreviations) recorded on the shell and genitalia.

Table S3. Genetic distance matrix (uncorrected distances in percentage) based on the amplified COI fragment for *Corrosella* species included in this study. Intraspecific genetic divergence is shown along the diagonal.

Supp. file 2. Supporting information. https://doi.org/10.5852/ejt.2026.1043.3203.14219

Fig. S1. Phylogenetic relationships among *Corrosella* species inferred using maximum likelihood based on the concatenated dataset of three gene fragments. Transfer bootstrap expectation (TBE) and Felsenstein bootstrap (FB) support values for key branches are represented by coloured squares. Scale bar below the topology indicates substitutions per site.

Fig. S2. Phylogenetic relationships among *Corrosella* species inferred using maximum likelihood and Bayesian inference based on the COI dataset, including *C. piti*. Transfer bootstrap expectation (TBE) and Bayesian posterior probability (BPP) support values for nodes above the species level are indicated by coloured squares. The scale bar below the topology represents substitutions per site.